Dictyostelium discoideum RnoA Interprets cAMP Mediated Signals to Influence Actin Organization

By

Rebecca Garcia

A dissertation submitted to the Graduate Faculty in Biochemistry in partial fulfillment of the requirements for the degree of Doctor of Philosophy, The City University of New York

2011

This manuscript has been read and accepted for the
Graduate Faculty in Biochemistry in satisfaction of the
dissertation requirements for the degree of Doctor of Philosophy

Derrick Brazill, Ph.D.

Date — Chair of Examining Committee

Edward Kennelly , Ph.D.

Date — Executive Officer

David Foster, Ph.D

Patricia Rockwell Ph.D.

Anne Bresnick Ph.D.

Peter Lipke Ph.D.

Supervisory Committee

THE CITY UNIVERSITY OF NEW YORK

ABSTRACT

Dictyostelium discoideum RnoA Interprets cAMP Mediated Signals to Influence Actin Organization

by

Rebecca Garcia

Adviser: Derrick Brazill, PhD

Tight control of actin cytoskeletal dynamics is essential for proper cell function. ARNO, a guanine nucleotide exchange factor for Arf, is associated with actin cytoskeletal regulation but its exact role is unknown. To explore ARNO's role in this regulation and in actin mediated processes, the *Dictyostelium discoideum* homolog RnoA was examined. RnoA is involved in development, as the reduction of RnoA by antisense prolongs aggregation, delaying development. Also, RnoA overproduction arrests development at the mound stage. This arrest is rescued by the addition of wild type cells. In these chimeric mixtures, *rnoA* overexpressing cells (RnoA OE) preferentially sort to the stalk, suggesting RnoA plays a role in cell sorting. RnoA antisense and RnoA OE cells fail to stream during aggregation. Chemotaxis assays reveal these mutants do not chemotax toward cAMP, indicating RnoA is part of the cellular response to cAMP. This defect is specific to cAMP-directed chemotaxis, as both RnoA mutants effectively chemotax to folate and exhibit normal cell motility. The chemotactic defects of the RnoA mutants may be due to an impaired cAMP response as evidenced by altered cell polarity and F-actin polymerization after cAMP stimulation. RnoA OE cells have increased filopodia compared to wild type cells, implying altered F-actin localization. Thus, RnoA likely organizes F-actin during development. Phospholipase D (PLD), the enzyme responsible for phosphatidic acid production, and paxillin, a cytoskeletal adaptor protein, are also involved in actin cytoskeletal

organization. Given their communal association with the actin cytoskeleton, we explored the interactions between RnoA and the *D. discoideum* PLD and paxillin homologs, PldB and PaxB, respectively. PaxB and PldB regulate calcium dependent and calcium independent cell-cell cohesion, respectively. Cells lacking PaxB are known to have reduced cell-substrate adhesion. We find that overexpression of PldB rescues the adhesion defect of *paxB* null cells, implying a genetic interaction between *paxB* and *pldB*. Co-immunoprecipitation studies suggest RnoA, PldB, and PaxB physically interact. This interaction does not depend on PaxB, PldB, or F-actin organization. Taken together, the results suggest that RnoA, in complex with PldB and PaxB, coordinates F-actin organization during actin mediated processes such as adhesion.

TABLE OF CONTENTS

LIST OF FIGURES

LIST OF TABLES

CHAPTER 1: Introduction

1.1 The actin cytoskeleton.

The highly dynamic actin cytoskeleton provides mechanical strength and morphology for the cell by serving as a mediator between the extracellular matrix and internal cellular machinery, thus enabling a cell to appropriately respond to external cues. Through reorganization in response to extracellular and intracellular signaling, the actin cytoskeleton plays an integral role in a variety of fundamental cellular processes including motility (99), adhesion (46), cytokinesis (59), and endocytosis (76). Given its extensive and complex role, the actin cytoskeleton is tightly regulated by various actin-binding proteins. Improper regulation of the actin cytoskeletal network is known to be a pivotal step in a cell's transition to malignancy. For instance, the actin cytoskeleton helps stabilize interactions between carcinoma cells and the extracellular matrix, a required step for cancer metastasis (28). In addition, alteration of a wide assortment of actin-binding proteins also facilitates disease progression. The actin-binding protein transgelin has tumor suppressive properties and its loss is observed in prostate, breast, and colon cancers (3) (66). Likewise, the misexpression of cortactin, an actin-binding adaptor protein, has been correlated with the progression of melanomas in human tissues (102). These findings suggest that the actin cytoskeleton, as well as actin associated proteins, plays a prominent role in disease development. As changes in actin-binding proteins influence the actin cytoskeletal network and thus actin-mediated processes, a thorough understanding of the signaling pathways governing cytoskeletal dynamics would yield great strides in elucidating actin-based physiological processes, particularly as these very processes are often exploited in diseased cells.

1.2 ARNO.

One regulator of actin cytoskeletal dynamics is ARNO (Arf nucleotide binding-site opener). ARNO, also known as cytohesin-2, is a member of the ARNO/cytohesin family of mammalian guanine nucleotide exchange factors (GEFs). GEFs catalyze the exchange of GDP for GTP, activating their target protein. ARNO serves as a GEF for Arf proteins, small GTP-binding proteins of the Ras superfamily known for their involvement in membrane trafficking (60). ARNO has been implicated in actin cytoskeletal rearrangements (25, 26), as well as the actin-based processes of cell motility (88), endocytosis (81), and exocytosis (92). In epithelial cells, the overexpression of ARNO results in changes in cell morphology and the formation of large lamellipodia, as well as the stimulation of cell motility (70). ARNO has also been shown to mediate neurite outgrowth and branching, processes dependent upon cytoskeletal coordination (30, 75, 103). Given the wide-range involvement of the actin cytoskeleton in cellular function, a detailed understanding of ARNO's role in actin-based processes, as well as its binding partners, can bring new insights about key players in the upstream regulation of the actin cytoskeleton and the mechanisms behind actin-dependent processes.

1.2.1 Structure.

ARNO is characterized by an N-terminal coiled-coiled domain, a central catalytic Sec7 domain, and a C-terminal pleckstrin homology (PH) domain (25). The coiled-coil domain mediates homodimerization and has been implicated in the localization of ARNO to the plasma membrane in polarized epithelial cells (81). The Sec7 domain, named for its homology to yeast protein Sec7, catalyzes the exchange activity of ARNO (9). The neighboring PH domain positively regulates this exchange activity through its interaction with inositol phospholipids (9).

1.2.2 Function and regulation.

ARNO acts as a GEF for the Arf family of small GTP-binding proteins. ARNO catalyzes the exchange of GDP for GTP to bring Arf to its active GTP bound state. Like other cytohesin family members, ARNO is promiscuous in its Arf activation. *In vitro* studies suggest that ARNO catalyzes the exchange of GDP for GTP to activate both Arf1 and Arf6 (25). Given their common localization to the plasma membrane, ARNO has been suggested to serve as a GEF for Arf6 (25) (9). The precise *in vivo* substrate for ARNO, however, remains controversial (16), indicating much remains to be understood concerning the complex relationship between Arfs and ARNO.

ARNO is known to play a role in actin cytoskeletal regulation through a variety of signaling pathways. Signaling through Arf6, ARNO catalytic activity alters the organization of the actin cytoskeleton. ARNO induces lamellipodia formation in epithelial cells, promoting separation from the epithelium and increased cell motility (70). Expression of catalytically inactive ARNO prevents actin reorganization and lamellipodia formation (26), suggesting ARNO's nucleotide exchange capabilities are essential for actin remodeling. In HeLa cells, ARNO has been shown to work in conjunction with PKC activation to reassemble actin to form broad lamellipodia (26). The enhanced cell motility associated with ARNO expression is a result of the downstream activation of both Rac and phospholipase D (PLD) pathways by ARNO (70). ARNO mediates Rac activation through the Rac GEF complex, Dock180/Elmo, though the mechanism of action remains to be elucidated (72). Similarly, the mechanism by which ARNO activates PLD has not yet been described. Uncovering the means by which ARNO activates its downstream targets can further expand our knowledge of actin cytoskeletal organization and the proteins involved in its regulation.

Due to its ability to regulate actin organization, ARNO has been linked to vesicular transport in a variety of cells. ARNO regulates clathrin-mediated endocytosis in polarized epithelial cells (81), calcium-mediated exocytosis in neuroendocrine cells (92), and endosomal trafficking in kidney proximal tubular epithelial cells (52). ARNO has again been associated with ELMO, along with β-arrestin, in the endocytosis and desensitization of G protein coupled receptors (GPCRs) (6, 15). Through adaptor molecules such as Elmo, ARNO may serve as a link between GPCRs and the actin cytoskeleton. For example, CaSR, a GPCR which senses extracellular calcium, promotes actin cytoskeletal reorganization leading to cell chemotaxis through a signaling network involving β-arrestin, ARNO, Arf6, and ELMO (6). Thus, ARNO appears to be at the forefront of communications between extracellular signals and the actin cytoskeleton to enable appropriate cellular responses.

While ARNO regulates the actin cytoskeletal network, ARNO is itself subject to regulation. ARL4D, a member of the Arf-like family of small GTPases, has been shown to regulate ARNO activity. The GTP activated form of ARL4D recruits ARNO to the plasma membrane through direct interaction with ARNO's PH domain (32). The localization of ARNO to the plasma membrane is followed by activation of its downstream target Arf6 and the loss of actin stress fibers, leading to cell motility (47). In mouse neuroblastoma cells, ARL4D is known to promote neurite outgrowth through the activation of ARNO and Arf6 (103). Phosphorylation of ARNO on key residues may also serve a regulatory role. PKC phosphorylation of ARNO on serine 392 in both *in vitro* and *in vivo* studies negatively regulates membrane localization (26, 71). As ARNO is recruited to the plasma membrane for activation, diminishing ARNO's affinity for membrane binding by the introduction of a phosphate group likely serves as a means of down regulating ARNO catalytic activity.

1.2.3 Protein interactions.

As mammalian ARNO has been associated to various actin-dependent processes, many different proteins may potentially interact with ARNO. One potential interaction partner is phospholipase D (PLD), the enzyme which catalyzes the hydrolysis of membrane-bound phosphatidylcholine to produce choline and phosphatidic acid (27). Phosphatidic acid, in turn, serves as a key second messenger in a variety of cellular processes. Like ARNO, PLD has also been functionally linked to the actin cytoskeleton and actin mediated processes such as vesicular transport, cell migration, and cancer development (36) (24). PLD plays a prominent role in cell adhesion of various cell types, including neutrophils and phagocytes (65) (35). ARNO is known to promote PLD activity during cell migration (70), exocytosis (92) (91), and after insulin stimulation (48). The PLD1 isoform and Arf6, the downstream target of ARNO, both colocalize to lamellipodia and membrane ruffles after antigen stimulation in rat basophilic leukemic cell lines (64) (68). PLD1 activity has also been found in cell membrane fractions containing regulatory proteins such as Arfs and the actin cytoskeletal protein paxillin (36). While a direct interaction has not been described, given their involvement in the same processes, in addition to their common localization, ARNO and PLD may potentially interact.

The adaptor protein paxillin may also interact with ARNO, as well as PLD. Paxillin localizes to focal adhesions and provides multiple docking sites for a variety of signaling molecules, including those involved with cytoskeletal rearrangements (17). By serving as a scaffold or adaptor for regulatory and structural proteins, paxillin is fundamental for the coordination of key components involved in actin cytoskeletal organization, adhesion, and motility (17). Given paxillin's role as an adaptor protein, paxillin interacts with numerous proteins from an assortment of signaling pathways. A variety of Arf GTPase activating proteins

(GAPs) are known to bind paxillin. For instance, the paxillin-binding PAG3 protein and its GAP target Arf6, mediate paxillin localization to focal adhesion sites (44). The ability of several Arf GAPs to bind paxillin suggests that tight regulation of Arf proteins is important for paxillin signaling (77). As ARNO serves as a GEF for Arf6, ARNO may also potentially be involved in paxillin localization. In addition, PLD1 has been reported to partially colocalize with paxillin in focal adhesion sites (35). The possibility of an ARNO-PLD-paxillin interaction is further supported by the finding that, like PLD, paxillin also colocalizes with ARNO to broad lamellipodia (70).

The localization of ARNO, PLD, and paxillin to areas of active actin remodeling, such as lamellipodia, enables each protein to play a prominent role in cell migration (**Figure 1**). Upon stimulation from a variety of extracellular factors such as potassium (92) and insulin (48), as well as wounding (70), ARNO activates Arf and PLD at the plasma membrane. Activation of these targets permits actin reorganization and in turn cell migration. Paxillin, also present in the vicinity, is phosphorylated in response to integrin binding and various growth factors including hepatocyte growth factor (HGF) (77). Phosphorylated paxillin mediates cross-talk between the varied signaling molecules associated with adhesion and motility, including members of the MAP kinase family (33) and the Rho-GTPase pathway (87), to promote cell motility. ARNO has also been proposed to lie downstream of HGF, activating cell migration through Arf and Rac (88). As paxillin also promotes migration through HGF signaling, ARNO and paxillin may function in the same pathway and perhaps even interact.

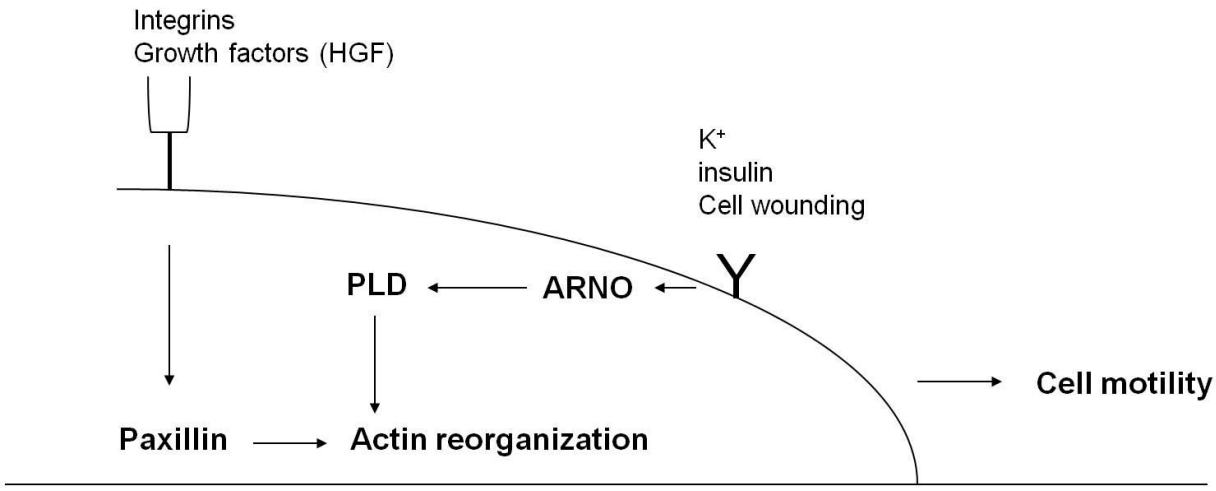

Figure 1: ARNO, PLD, and paxillin regulate actin cytoskeletal changes to enable cell motility. Upon stimulation by wounding or various factors, ARNO activates PLD activity. Extracellular factors also promote paxillin phosphorylation. PLD activity and paxillin phosphorylation lead to reorganization of the actin cytoskeleton, allowing cell motility to occur.

The functional association of ARNO, PLD, and paxillin to the actin cytoskeleton and its mediated processes highlights the potential for a protein complex containing catalytic PLD properties, regulatory proteins such as Arfs, and adaptor proteins such as paxillin (36). Such a complex may play an intimate role in the coordination and regulation of actin cytoskeletal organization required for processes such as adhesion and motility. The precise mechanism of interaction of these proteins and the role of ARNO in this potential protein complex remains to be elucidated.

1.2.4 *D. discoideum* ARNO.

The *Dictyostelium discoideum* genome contains a single gene homologous to mammalian ARNO. Given its homology to ARNO, the protein encoded by the 2961 nucleotide *secG* gene (Dictybase ID DDB091439), which resides on chromosome 5, was named RnoA. Like mammalian ARNO, the predicated 107 kD RnoA has a putative catalytic Sec7 domain and a C-

terminal pleckstrin homology (PH) domain (**Figure 2A**). Together, these domains share 61% similarity and 44% identity to *Homo sapiens* ARNO (**Figure 2B**). The C-terminal domain of *D. discoideum* RnoA also contains the same series of positively charged residues present in ARNO. In addition, RnoA possesses a series of N-terminal ankyrin repeats which are absent in ARNO. Ankyrin repeats are known to mediate protein-protein interactions (56).

RnoA contains two highly conserved sequence motifs present in Sec7 domains from ARNO orthologs from various species (**Figure 2B**). These motifs form the sides of the hydrophobic pocket where Arf1 binds to ARNO *in vitro* (13). Five residues in these motifs, Arg 152, Glu 156, Met 194, and Asn 201, have been shown to be vital for Sec7 catalytic function in ARNO (13). All five of these residues are conserved in RnoA's Sec7 domain, suggesting that RnoA likely retains nucleotide-exchange capabilities.

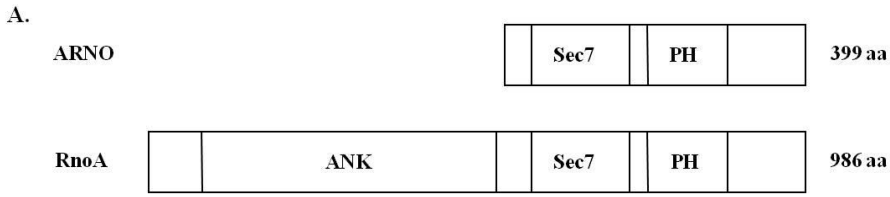

B. Sec7 domain

```
ARNO    EERMELENIRRRKQELLVEIQRLREELSEAMSEVEGLFANEGSKTLQRNRKMAMGRKKFNMDPKKG  79
        +E  ++ N R      + E+Q   E+  +A  ++E L A E  K L     +A    +FN  PKKG
RnoA    DEIYQIVNKRESSNHEVDELQLALEQ--QAKEDMEQLAA-EKQKLLLIKAAIA----QFNSHPKKG 605

ARNO    IQFLVENELL-QNTPEEIARFLYKGEGLNKTAIGDYLGEREELNLAVLHAFVDLHEFTDLNLVQAL 144
        I+F+V N ++ +  P+E+A FL     L+K +IG+Y+GE ++ NL VLHAFVD   F  L+   AL
RnoA    IEFIVANGVISEKNPKEVAHFLLTHSELSKQSIGEYIGEGDDFNLQVLHAFVDELNFFGLDFDVAL 671
                motif 1                                  motif 2
ARNO    RQFLWSFRLPGEAQKIDRMMEAFAQRYCLCNP--GVFQSTDTCYVLSFAVIMLNTSLHNPNVRDKP 208
        R++L +FRLPGEAQKIDRMME FA ++   NP   VF + D  YVL+F+VIMLNT  HNPN++ K
RnoA    RKYLLTFRLPGEAQKIDRMMEKFASQFYQHNPKENVFVNQDAVYVLAFSVIMLNTDAHNPNIKKKM 737

ARNO    GLERFVAMNRGINEGGDLPEELLRNLYDSIRNEPFKIPEDDG 250
            F+  N GIN G DLP + + NLYD I      K+ E DG
RnoA    TKAEFLRNNSGINSGDDLPPDFMENLYDKIVTNEIKM-ERDG 778

        PH domain

ARNO    NDLTHTFFNPDREGWLLKLGGRVKTWKRRWFILTDNCLYYFEYTTDKEPRGIIPLENLSIREVDDP 316
        N       + +++GWL K GGR+KTWK+RWFILT NCL Y++   D EP GIIPLEN+ +    DP
RnoA    NQANQ---HVEKKGWLTKQGGRIKTWKKRWFILTANCLLYYKTPQDHEPCGIIPLENVVV--TIDP 839

ARNO    RKPNCFELYIPNNKGQLIKACKTEADGRVVEGNHMVYRISAPTQEEKDEWIKSIQAAVSVDPFYEM 382
        +K  CF L+   +  + +KACK  +DG +V+ NH  Y I+A    E D W++SI ++ +  +P +E
RnoA    QKKFCFMLH---SSQEQMKACKLNSDGTLVQANHAAYFIAAANMAEMDSWVQSIKSNIHSNPNFEQ 902

ARNO    LAARK  387
        L  RK
RnoA    LLKRK  907
```

Figure 2: ***Dictyostelium discoideum*** **RnoA is homologus to mammalian ARNO.** (A) *Homo sapiens* ARNO features a catalytic Sec7 domain and a C-terminal PH domain. Both the Sec7 domain and the PH domain are present in the *Dictyostelium discoideum* homolog RnoA. RnoA also contains an additional N-terminal ankyrin repeat domain (ANK). (B) The catalytic Sec7 domain and PH domain of RnoA share high sequence identity and similarity (shown in bold and by +, respectively) to *H. sapiens* ARNO. Two Sec7 domain motifs (motif 1 and motif 2) thought to play a role in substrate binding are conserved in RnoA.

1.3. *Dictyostelium discoideum*.

The eukaryote *Dictyostelium discoideum* boasts a multitude of properties that presents this organism as an ideal model system. The completely sequenced 35-Mb genome contains many mammalian protein homologs, including 33 homolgous to diseased-linked proteins (98) (22). *D. discoideum* provides an excellent model for investigating the interactions between Arfs and ARNO as many mammalian signal transduction pathways remain conserved in this organism. Many Ras superfamily proteins have been observed to participate in actin-related processes in *D. discoideum*, including a variety of GTPases, GEFs, and GAPs (49). The *D. discoideum* genome contains a total of sixteen Arf, Arf-related, and Arf-like proteins and components of the Arf signaling cascade appear to be conserved in this organism (55). In addition, a wide assortment of molecular genetic tools has been established in *D. discoideum* including random insertational mutagenesis, RNA interference methodologies, and homologous gene replacement (23). *D. discoideum* is readily grown in clonal cell cultures on nutrient agar plates or in suspended nutrient media. Cells in liquid culture exhibit a rapid 8-10 hour replication time. Removal of nutrients triggers a developmental program characterized by a cooperative behavior that results in multicellular organization within 24 hours. Thus, the properties of cells in a multicellular state, as well as the physiological role of specific proteins in a multicellular system, can readily be observed in *D. discoideum*.

1.4 *D. discoideum* life cycle.

Dictyostelium discoideum rely on a variety of actin dependent processes during both growth and developmental stages, including adhesion, motility, chemotaxis, and phagocytosis. During the growth phase, *D. discoideum* live as individual cells that feed through phagocytosis

and undergo cell division. These amoebe hunt their bacterial prey by chemotaxis using the folic acid produced by bacteria as a chemoattractant (63). In the absence of a food source, cells undergo starvation and transition from the single-celled vegetative state to multicellular development (**Figure 3**).

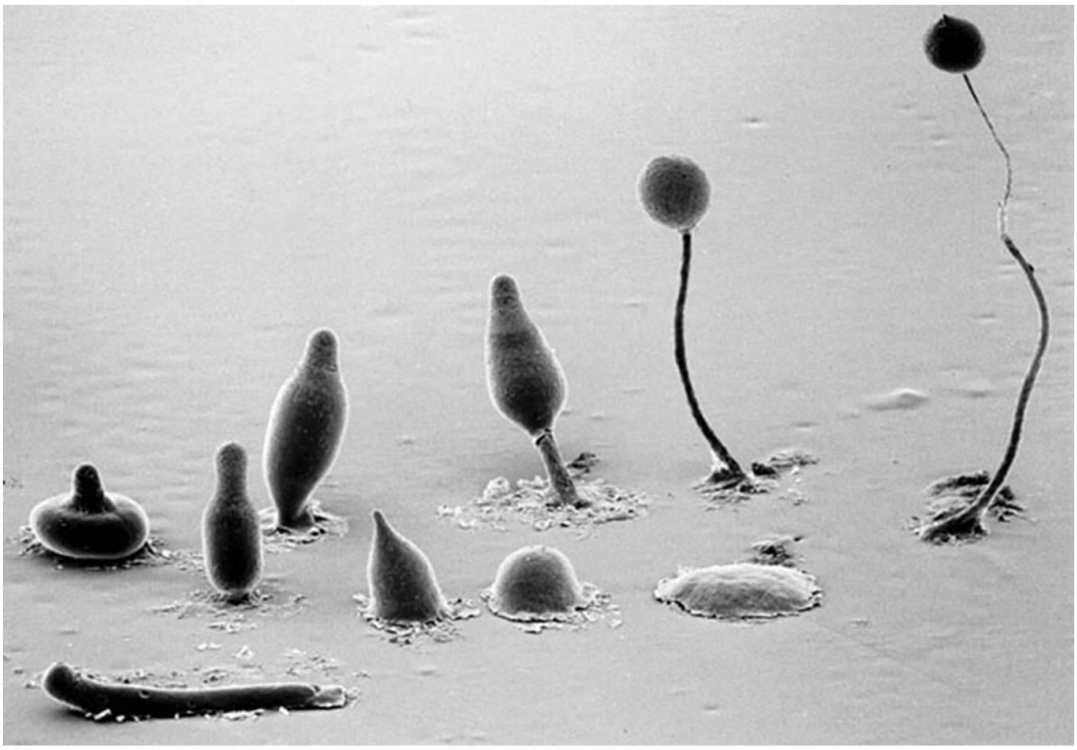

Figure 3: The developmental cycle of *Dictyostelium discoideum.* As *D. discoideum* undergo starvation, cells enter into multicellular development encompassing several stages that lead to fruiting body formation. Moving clockwise from the bottom right, cells transition through the loose aggregate, the tight aggregate or mound, the tipped mound, the finger, the slug (lower left), and the culmination stages from the Mexican hat to the fruiting body. Scanning electron image copywrite, M.J. Grimson and R.L. Blanton, Biological Sciences Electron Microscopy Laboratory, Texas Tech University.

As starvation begins, expression of genes involved in cell aggregation occurs, including those needed to produce and secrete cAMP (41) (73). cAMP is released by starving cells and replaces folic acid as a chemoattractant during development, enabling neighboring cells to migrate toward the largest population of starving cells (73) (4) (53). Proper actin cytoskeletal organization is

crucial for cAMP-responsive cells to become polarized along the cAMP gradient and orient themselves in a head-to-tail fashion, forming streams that give rise to multicellular aggregates known as mounds (45). The cells within each aggregate undergo cell sorting and differentiation into prespore and prestalk cells, depending upon their ability to respond to cAMP (34) (1) (95). The complex process of cell sorting involves chemotaxis and adhesion, both actin-mediated processes. Cell sorting places prestalk cells at the mound tip, which extends into a finger-like projection. Fingers commonly fall sideways and migrate as a single entity, known as a slug, in response to heat and light sources, processes termed thermotaxis and phototaxis, respectively (18). The actin cytoskeleton and a variety of proteins commonly associated with the cytoskeleton are important for phototaxis (42). Slugs are characterized by a precise spatial patterning of prestalk cells at the anterior and prespore cells at the posterior (51). Culmination occurs as slugs transition into fruiting bodies. A subtype of the prestalk cells migrates toward the substratum and generates the vacuolated stalk, gradually pushing the prespore cells upward (41) (18). The developmental cycle is completed upon the formation of a fruiting body, consisting of dead stalk cells supporting a mass of viable spore cells on top. Spores remain in a dormant state until adequate nutrients become available, permitting germination. Evidence suggests that actin reorganization plays a role in maintaining spore dormancy and viability until the appropriate conditions arise (69). From phagocytosis in the vegetative state, to cell sorting in the mound stage, and spore preservation in the fruiting body, the actin cytoskeleton and its tight regulation is vital in all life stages of *D. discoideum*.

1.5 Significance.

Regulation of the actin cytoskeleton is essential for many fundamental cellular processes. A multitude of proteins and signal transduction pathways converge to orchestrate actin cytoskeletal dynamics in mammalian cells, complicating the analysis of a single protein's contribution to this system. The mammalian protein ARNO has been implicated in the regulation and organization of the actin cytoskeleton. The precise role of ARNO in this regulation, as well as binding partners for ARNO, has not yet been elucidated. Two potential interaction partners include the enzyme phospholipase D (PLD) and the adaptor protein paxillin, both of which have prominent roles in the development and progression of cancer. Knowledge of the relationship between ARNO, PLD, and paxillin can illuminate greater detail on ARNO's physiological role as well as bring new understanding about the key players in cancer metastasis. Given the complexity of mammalian signaling pathways, exploring the signaling events surrounding ARNO, PLD, and paxillin in a less convoluted system such as *D. discoideum* can minimize crosstalk among different pathways.

In this work, we demonstrate a role for RnoA, the *Dictyostelium discoideum* homolog of ARNO initially termed SecG, in cAMP mediated actin organization. We show that RnoA is involved in *D. discoideum* development by integrating cAMP signaling with actin cytoskeletal reorganization. In addition, we show that RnoA forms a complex with PldB and PaxB, homologs of phospholipase D and paxillin, respectively. The knowledge gained can be applied to the homologs of RnoA, PldB, and PaxB in mammalian cells to bring new insights regarding the involvement of these proteins in actin-based processes, which are fundamental for cell survival.

CHAPTER 2: Materials and methods

2.1 Cell culture and development.

Dictyostelium discoideum wild type Ax2 cells were grown axenically in HL5 medium at 22°C in shaking culture (85). Ax2 cells carrying the endogeneous MB35 plasmid (Tet7) were grown in HL5 supplemented with 5 µg/ml G418. Ax2 cells expressing β-galactosidase (HR30) were grown in HL5 supplemented with 20 µg/ml G418. RnoA overexpressing cells (RnoA OE) and RnoA antisense cells were grown in HL5 supplemented with 20 µg/ml G418 and 10 µg/ml Blasticidin S. For development, 1 x 10^7 cells in mid-log phase (2-5 x 10^6 cells/ml) were washed with PBM (20 mM KH_2PO_4, 0.01 mM $CaCl_2$, 1 mM $MgCl_2$, pH 6.1 with KOH), plated onto filter pads, and then incubated at 22°C (37). For development on agar, wild type cells were grown on a lawn of *Klebsiella aeruginosa* while mutant strains were grown on a lawn of G418 resistant *Escherichia coli*.

2.2 Generation of RnoA antisense cell lines.

The tetracycline-inducible system described by Blaauw et al (5) was utilized to diminish RnoA levels in *D. discoideum*. Nucleotides 51 to 795 were digested from the full length *rnoA* gene utilizing the EcoRV and AatII restriction sites. The MB38 vector was linearized with BglII restriction digestion. To generate blunt ends, the linearized MB38 vector was incubated with 1U Klenow fragment (New England Biolabs Ipswich, MA), 33 µM dNTPs (Calbiochem San Diego, CA), and 1x NEB buffer #4 for 15 minutes at room temperature, followed by quenching with 10 mM EDTA. After Klenow treatment, the 700bp fragment of the *rnoA* gene was then inserted in the antisense orientation into the MB38 plasmid through the BglII and EcoRV restriction sites.

This plasmid was then transformed into Tet7 cells and transformants were selected on GYP plates containing 10 µg/ml Blasticidin S and 20 µg/ml G418.

2.3 Chimeras and β-galactosidase staining.

Chimeras were generated following the protocol described by Jermyn and Williams (38) with slight modifications. Briefly, 9 x 10^6 wild type or mutant cells and 1 x 10^6 HR30 cells were harvested and washed three times with PBM. Chimeras consisted of 10% HR30 and 90% wild type or mutant cells were developed on white filter pads, 0.8 µm pore size (Millipore, Billerica, MA). Fruiting body structures were fixed with glutaraldehyde solution (1 ml 25% glutaraldehyde solution and 0.25 ml Triton X-100 in Z Buffer (60 mM Na_2HPO_4, 40 mM NaH_2PO_4, 10 mM KCl, and 1 mM $MgSO_4$)) and then stained with X-gal solution (5 mM $K_3[Fe(CN)_6]$, 0.4 mg/ml X-gal, and 0.5% Tween 20 in Z Buffer). After overnight incubation at 37°C, images were taken with a dissecting microscope utilizing the SPOT Advanced program and the SPOT insight color camera (Diagnostics Instruments, USA).

2.4 Low cell density assay.

Cells were starved at 22°C for 16 hrs in submerged monolayer culture at densities of 224 x 10^3, 112 x 10^3, 56 x 10^3, 28 x 10^3, 14 x 10^3, and 7 x 10^3 cells/cm^2 in PBM. Images were taken with an inverted Nikon TE 200 Eclipse microscope using Metamorph Image System (Molecular Devices, Downingtown, PA) viewed with a 10x objective.

2.5 Chemotaxis assay.

Under agarose chemotaxis assays were performed as described by Woznica and Knect (101), with some adjustments. For cAMP chemotaxis, 1 x 10^7 cells were starved on filter pads for 5 hrs. Cells were collected and resuspended in 1 ml PBM. A 100 µl sample of cells was used in the assay. For folate chemotaxis, vegetative cells were collected and resuspended to 1 x 10^6 cells/ml and 100 µl used in the assay. Images of cells migrating under agarose toward 10 µM cAMP or 1 mM folate were taken every 30 sec for 20 min on an inverted Nikon TE 200 Eclipse microscope using Metamorph Image System (Molecular Devices, Downingtown, PA) viewed with a 10x objective. Cells were tracked with Image J software. Directionality is defined as (absolute distance traveled)/ (total path length), where a maximum value of 1 represents a straight path without deviations. The chemotactic index is determined by calculating the cos θ, where θ represents the angle of deviation between a straight line up the chemotactic gradient and the net path of a cell. A value of 1 is equivalent to a straight path up the chemotactic gradient.

2.6 Cell motility assay.

1 x 10^6 cells were collected, washed with PBM, and resuspended in 10 ml PBM. 200 µl of cells were placed into a 24 well plate with 200 µl PBM. Cells were starved for 6 hrs. cAMP was then added to the cells for a 5 µM final concentration. Images of cells in the absence and presence of cAMP were taken every 30 sec for 20 min on an inverted Nikon TE 200 Eclipse microscope using Metamorph Image System (Molecular Devices, Downingtown, PA) viewed with a 10x objective. Cells were tracked with Image J software.

2.7 Cell polarization assay.

A cAMP gradient was established as described by Woznica and Knect (101), with some modifications. Briefly, PBM + 0.75% agarose was poured into a 4-well Millicell EZ slide (Millipore, Cork, Ireland). After solidifying, the agarose was removed from half of each well. Using a pipet tip, a small well was made 5 mm from the edge of the agarose. The well was then filled with 10 µM cAMP + 20 mg / ml FITC-dextran (Sigma, St. Louis, MO) and a gradient was allowed to develop. 5 hr starved cells were then placed onto the slide for approximately 1×10^4 cells/ cm^2. Establishment of the cAMP gradient and was confirmed on an inverted Nikon TE 200 Eclipse microscope using Metamorph Image System (Molecular Devices, Downingtown, PA) viewed with a 10x objective. Cells were then fixed and stained for actin as described above. Images were taken on a Leica confocal microscope. Cell circularity was measured utilizing Image J software.

2.8 F-actin polymerization assay.

For F-actin polymerization in response to folate, 5×10^7 cells in the vegetative state were washed with PBM and resuspended in 10 ml PBM for 5×10^6 cells/ml. After shaking for 30 min, cells were washed and resuspended in 1 ml PBM. Cells were stimulated with 50 µM folate. 100 µl samples were collected after 0, 5, 10, 20, and 60 seconds and placed into 500 µl actin fixative buffer (10 mM PIPES, pH 6.8, 20 mM K_2HPO^4, 5 mM EGTA, 0.5% Triton X, 3.7% formaldehyde, 0.25 mM AlexaFluor Phalloidin 488). For F-actin polymerization in response to cAMP, 1×10^7 cells were starved for 5 hrs on filter pads. The cells were then collected, washed with PBM, and resuspended to 2ml PBM. Cells were stimulated with 1 µM cAMP. 100 µl

samples were collected after 0, 5, 10, 20, 30, 40, 50, 60, 80, 100, and 150 seconds and placed into 500 µl actin fixative buffer.

The samples were incubated in the dark for 1 hr and then centrifuged at 1300 rpm for 10 min at 4 °C. The supernatant was removed and the pellet resuspended in 1 ml methanol. The samples were incubated at 4 °C on a rotatory shaker overnight. 100 µl of each sample was placed onto a plate reader for measurement of fluorescence.

2.9 Actin staining.

Cells were washed twice with PBM and starved on an 8 well chambered slide for 6 hrs. Cells were fixed (3.7% formaldehyde in PBS for 5 min), washed with PBS, permeabilized (0.5% Triton X-100 in PBS), and washed with PBS. Cells were incubated with 100 µg/ml RNaseA for 1 hr. After a PBS wash, cells were stained with 8 U/ml Rhodamine Phalloidin (Invitrogen Eugene, OR) for 1hr in the dark. After a PBS wash, cells were incubated with 20 µM To-Pro (Invitrogen Eugene, OR) for 15 min. Slow Fade Gold (Invitrogen Eugene, OR) mounting solution was added prior to placing a coverslip onto the slide.

2.10 Western blot analysis.

The synthetic peptide GCEQLLKRKAETIRGRGKVS, corresponding to amino acids 901 to 918 in the C-terminal portion of RnoA, was utilized to immunize a rabbit at Biosynthesis, Inc (Lewisville, Tx). Serum was collected 8 weeks after the second injection and column purified using the above peptide. Cells were collected and boiled for 3 min in SDS-PAGE sample buffer. Proteins were separated by SDS-PAGE, transferred onto Hybond-P membranes

(Amersham Bioscience, Piscataway, NJ), immunoblotted with α-RnoA antibody, and visualized with enhanced chemiluminescent substrate for HRP detection (PIERCE, Rockford, IL).

2.11 Co-immunoprecipitations.

1 x 10^7 cells were lysed in 0.5 ml lysis buffer (20 mM HEPES pH7.5, 150 mM NaCl, 1.5 mM $MgCl_2$, 1 mM EGTA, 10% glycerol, 1% Triton X 100, 2x Roche Complete Protease Inhibitor Cocktail, Mini (Indianapolis, IN)). Samples were centrifuged at 4000 rpm for 5 min at 4°C and the pellet discarded. Cell lysates were incubated with 1 µg antibody overnight on a rotating shaker at 4°C. Pure Proteome Protein A magnetic beads (Millipore Temecula, California) were added to the sample and incubated on a rotatory shaker for 1hr at 25°C. Beads were collected with a magnetic rack (Millipore Temecula, California) and washed 3 times with PBS + 0.1% Tween. Beads were resuspended in 50 µl PBS + 0.1% Tween and 10 µl 6x sample buffer, then boiled for 10 min at 90°C. Beads were then removed from suspension with the magnetic rack.

For experiments involving Latrunculin A, samples were incubated with Latrunculin A (BIOMOL International Plymouth Meeting, PA) for 40 minutes on a rotatory shaker at room temperature prior to immunoprecipitation.

2.12 Cell-substrate adhesion assay.

Cell-substrate adhesion was performed as described by Chen and Katz (10) with slight modifications. A suspension of 1 x 10^6 cells in 1 ml of PBM was placed in a 125 ml glass culture flask and put on a gyratory shaker for 10 min at 120 rpm. The cells were allowed to adhere to the glass substrate for 2 hrs. The flask was then gently agitated for 3 min at 60 rpm.

The supernatant was collected and the number of cells present was counted with a hemacytometer.

2.13 Cell-cell cohesion assay.

The cell-cell cohesion assay was performed as described by Secko et al (79) with some adjustments. Exponentially growing cells were collected and washed three times in PBM then resuspended to 2 x 10^7 cells/ml. 2 ml were aliquotted into a 50 ml centrifuge tube and starved for 4 hours in horizontal suspension (175 rpm) at 22°C. 2.5 x 10^6 cells were collected and vigorously vortexed to disrupt cell aggregation. The cells were placed in a total volume of 2 ml in the absence or presence of 10 mM EDTA and then allowed to aggregate on a platform shaker at 140 rpm at room temperature. Cells were collected after 5, 20, 40, and 60 minutes. Single and duplex cells were then counted with a hemacytometer.

CHAPTER 3: RnoA plays a role in mound stage development

3.1 RnoA has peak production during development.

Mammalian ARNO is known to play a role in various actin dependent processes such as motility, as well as in actin cytoskeletal organization. *Dictyostelium discoideum* heavily relies on actin mediated processes throughout its development. To determine if the *D. discoideum* homolog of ARNO, known as RnoA, also influences actin organization and actin dependent prcesses, the involvement of RnoA in development was assessed. In *D. discoideum*, the expression pattern of a protein is commonly correlated to its developmental function. Protein expression at a particular developmental stage may indicate this protein plays a role in the various processes occurring during that stage of development. To explore the protein expression pattern of RnoA, cell lysates from each stage of development were harvested. A Western blot was then performed on the lysates utilizing antibodies raised against a C-terminal peptide of RnoA in order to detect the presence or absence of RnoA at each developmental stage. As can be seen in **Figure 4**, RnoA is present throughout both vegetative and developmental stages. RnoA levels decrease as cells enter development and remain low during the initial stages of development. Maximum production of RnoA occurs approximately 12 hours into development, when cells undergo aggregation to form mounds. As development progresses beyond this mound stage into the generation of fingers and early culminants at 16 and 20 hours, respectively, RnoA levels again decrease. By 24 hours after the onset of development, when the formation of fruiting bodies completes the developmental cycle, RnoA is barely detectable. As RnoA levels vary throughout development, RnoA production is developmentally regulated, with peak production of RnoA occurring during the mound stage.

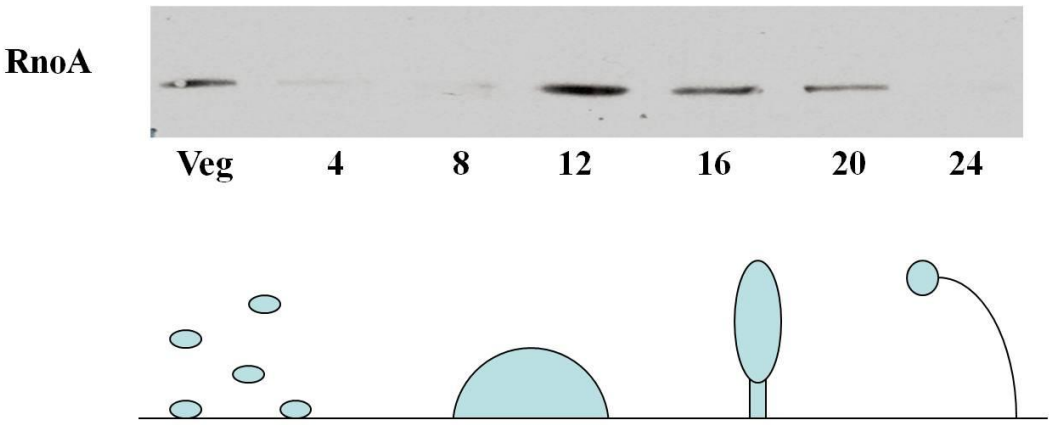

Figure 4: RnoA developmental protein expression in wild type cells. 1 x 10^7 cells were collected from wild type cells at different developmental stages. After separation by SDS-PAGE, proteins were identified by Western blotting with anti-RnoA antibodies.

3.2 Generation of RnoA mutants using the Tet-off sytem.

Cell lines with altered RnoA levels can be utilized to gain a better understanding of RnoA's role in development, as deviation from wild type phenotypes indicates the involvement of RnoA in a specific process or stage of development. In an effort to generate cell lines lacking RnoA, attempts were previously made to disrupt *rnoA* expression. As the total loss of RnoA did not yield viable cells, *rnoA* may be essential to cell survival and its absence may potentially be lethal. Therefore, the Tet-off system described by Blaauw et al (5) was utilized to reduce the expression of *rnoA*. This two vector system consists of the chromosomally integrated MB35 vector and the extrachromosomal response plasmid MB38. The integrated MB35 vector harbors a tetracycline-controlled transciptional activator (tTA) driven by an actin15 promoter. The extrachromosomal MB38 vector contains an inducible promoter comprised of a minimal promoter regulated by a tetracycline responsive element (TRE). In the absence of tetracycline, the tTA binds TRE to activate the minimal promoter, resulting in gene expression. Addition of

tetracycline halts gene expression by inducing a conformational change that prevents tTA from binding TRE, thereby silencing the promoter.

To generate a cell line with reduced *rnoA* expression, 700 base pairs of the *rnoA* gene were ligated into the MB38 vector in the antisense orientation as depicted in **Figure 5**. To confirm a reduction in RnoA production, the level of RnoA in RnoA antisense cell lysate was compared to RnoA levels in lysates from wild type cells and previously generated RnoA overexpressing (RnoA OE) cells. To ensure equal loading of each sample, the intensity of each RnoA band was normalized with actin by densitometry. As seen in **Figure 6**, Western blots probed for RnoA indicate a 1.5 fold reduction in RnoA production in the RnoA antisense cells, as compared to endogenous levels in wild type cells. The previously generated RnoA OE cells were found to have a 1.5 fold increase in RnoA production compared to wild type cells. Thus, a cell line with decreased levels of RnoA has now been produced.

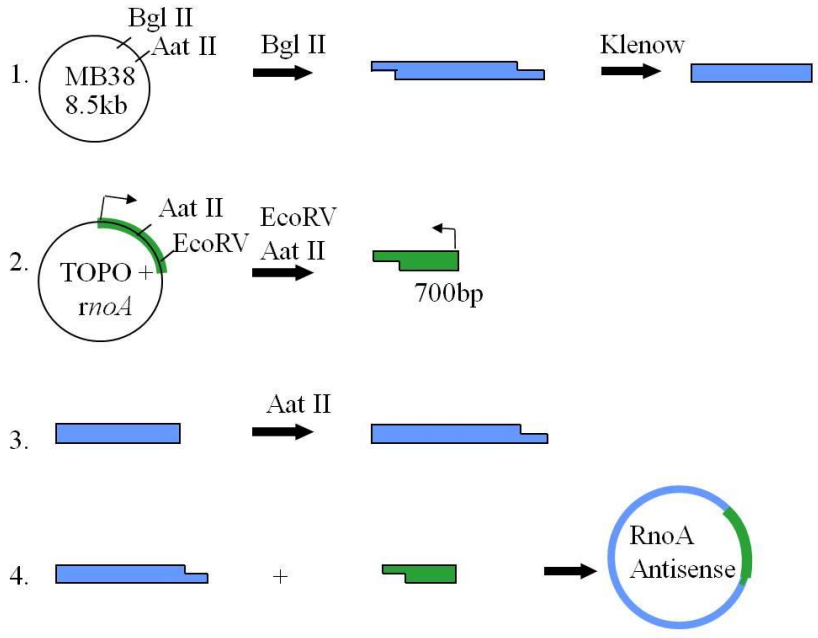

Figure 5: RnoA antisense construct design. A 700bp fragment of the *rnoA* gene was ligated in the antisense orientation into the MB38 plasmid.

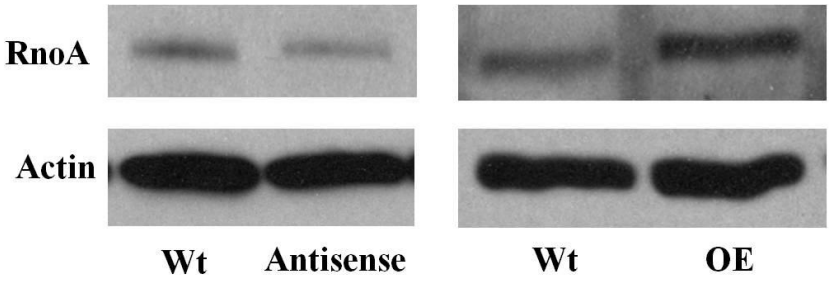

Figure 6: RnoA expression in wild type and mutant cell lines. 1 x 10^7 cells were collected from wild type (Wt) and RnoA antisense (Antisense) cells as well as RnoA over-expressing (OE) cells. After separation by SDS-PAGE, RnoA proteins were identified by Western blotting with anti-RnoA antibodies. To ensure equal loading, actin was detected with anti-actin antibodies and quantified by densitometry.

3.3 RnoA OE cells arrest at the mound stage.

As evidenced by its developmental expression pattern, RnoA likely plays a role during *D. discoideum* development. RnoA may possibly be involved during the mound stage of development as peak protein expression occurs during this stage. The influence of RnoA on development was explored by observing phenotypic differences between cells with altered RnoA production and wild type cells. Wild type and RnoA OE cells were seeded onto a bacterial lawn and allowed to develop. Wild type cells fully complete the developmental cycle and form fruiting bodies. RnoA OE cells, however, arrest at the mound stage of development, the stage after which RnoA levels drastically decrease (**Figure 7**). RnoA OE cells do not progress beyond the mound stage after any additional time. Thus the over production of RnoA disrupts normal development by preventing development past the mound stage.

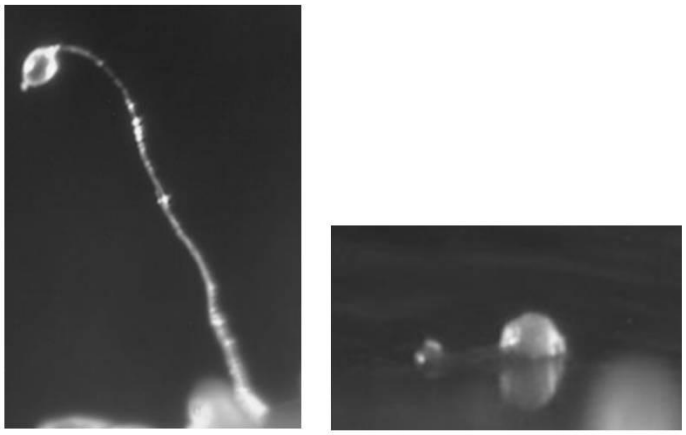

Figure 7 : RnoA OE cells arrest at the mound stage. Wild type (WT) and RnoA over-expressing (RnoA OE) cells were seeded onto a bacterial lawn over agar and allowed to develop. Bar, 0.1 mm.

3.4 RnoA OE cells preferentially localize to the stalk in chimeric mixtures.

To assess whether the presence of wild type cells could rescue the developmental defects of RnoA OE cells, chimeric mixtures of mutant cells and wild type cells expressing β-galactosidase (HR30 cells) were plated onto filter pads and allowed to develop. HR30 cells stain blue in the presence of X-GAL, allowing them to be identified in the fruiting body. The localization of the mutant cells in the fruiting body can be inferred by identifying the unstained cells. Addition of 10% HR30 cells to RnoA OE cells allows fruiting body formation, rescuing the developmental arrest of RnoA overexpression (**Figure 8**).

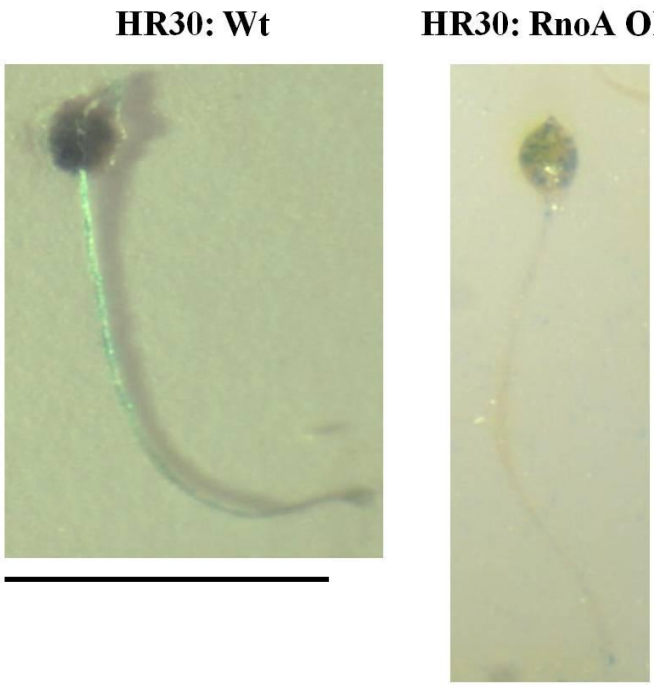

Figure 8: RnoA OE cells localize to the stalk in chimeric mixtures. 9 x 10^6 wild type (WT) or RnoA OE cells and 1 x 10^6 HR30 cells, wild type cells expressing β-galactosidase, were harvested and washed three times with PBM. Chimeras consisted of 10% HR30 and 90% wild type or mutant and were allowed to develop on filter pads. Chimeras were stained, fixed, and incubated overnight 37°C. Bar, 0.5 mm.

This suggests RnoA OE cells are able to respond to signals produced by wild type cells, but are unable to produce these signals themselves. RnoA therefore likely plays a non-cell autonomous role in development. To examine the localization of the HR30 cells in the fruiting body, chimeras were stained with X-GAL. Wild type cells mixed with HR30 cells have an even distribution throughout the fruiting body structure. This indicates that the expression of β-galactosidase in the HR30 cells does not influence cell sorting or differentiation. When mixed with RnoA OE cells, HR30 cells predominately localize to the spore mass and are absent from the stalk. Thus, the unstained cells in the stalk represent the RnoA OE cells. The unequal distribution of HR30 cells and RnoA OE cells suggests that the overproduction of RnoA causes defects in cell sorting. Taken together, the data suggest RnoA plays a non-cell autonomous role

in development as the addition of 10% wild type cells is sufficient to restore normal fruiting body development. Furthermore, elevated levels of RnoA appear to disrupt cell sorting as RnoA OE cells mainly localize to the stalk. Therefore, RnoA may potentially play a role in cell sorting or cell differentiation.

3.5 RnoA antisense cells are developmentally delayed.

To examine the effects of reduced RnoA levels on development, the developmental progression of RnoA antisense cells was compared to wild type cells. Wild type and RnoA antisense cells were plated onto filter pads and images were taken as cells progressed through development. Like its overexpression, the loss of RnoA also results in a defective developmental phenotype. RnoA antisense cells display a severe developmental delay with a prolonged aggregation stage. While wild type cells form large aggregates 4 hours into development, RnoA antisense cells are only beginning to form small aggregates (**Figure 9**). By 24 hours, these mutants are still at the aggregate stage while wild type cells have developed into fruiting bodies. RnoA antisense cells eventually form smaller, undersized fruiting bodies after 36 hours of development. Taken together, the data suggest RnoA plays a role in development as alterations in its endogenous expression lead to deviations from typical fruiting body formation. RnoA appears to be particularly important for mound stage development as the loss of RnoA leads to elongation of the aggregation stage and the overexpression of RnoA blocks any development past the mound stage.

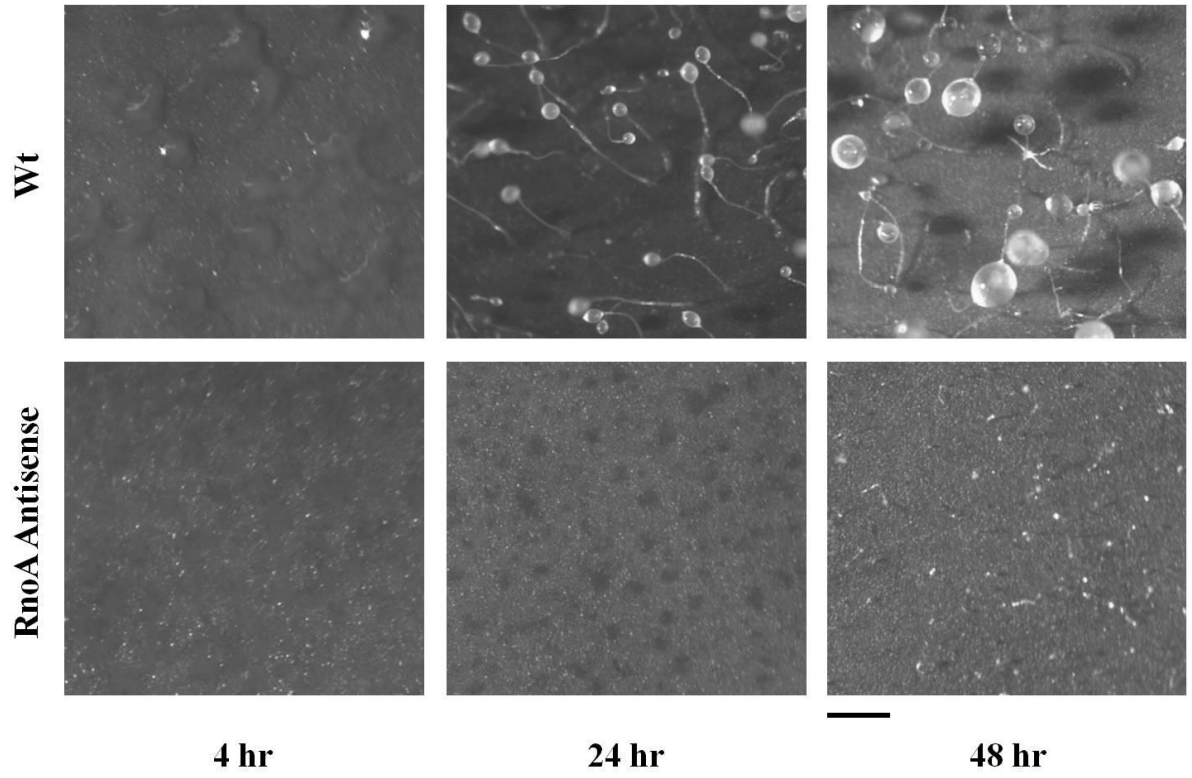

Figure 9: RnoA antisense cells are developmentally delayed. 1 x 10^7 cells were plated onto filter pads soaked in PBM buffer and allowed to develop. Images were taken at indicated time points. Bar, 0.5 mm.

3.6 Discussion.

RnoA is the *D. discoideum* homolog of ARNO, a known regulator of actin cytoskeleton organization. RnoA is present during both vegetative and developmental stages of *D. discoideum*. Expression of RnoA drops as vegetative cells enter the initial stages of development. As cells undergo the actin mediated processes of chemotaxis and cell streaming to aggregate and form mounds, RnoA is highly expressed. After the mound stage, when cells have differentiated and sorted according to cell-type, RnoA levels decline and culmination of fruiting bodies ensues. This suggests that RnoA is required during aggregation and mound formation, but needs to be removed after the mound has formed. Consistent with this, we find that both the overproduction and reduction of RnoA result in abnormal developmental phenotypes. Cells with

reduced RnoA levels have delayed development due to an extended aggregation stage. It is possible that high levels of RnoA are required for aggregation to occur. As the RnoA antisense cells have decreased levels of RnoA, it may take longer for these cells to achieve the levels of RnoA needed to undergo aggregation, thus delaying aggregation. RnoA OE cells arrest at the mound stage of development, the point after which RnoA levels decrease. It is possible that the RnoA OE cells arrest at the mound stage because RnoA levels never decrease. The artificially elevated levels of RnoA likely prevent progression to the next developmental stage.

Chimeric mixtures of RnoA OE cells and wild type cells demonstrated that the mound stage arrest of the RnoA OE cells can be rescued by the addition of 10% wild type cells. This finding implies that cells overexpressing RnoA are able to respond to developmental signals produced by wild type cells, but are unable to produce those signals themselves. Thus, RnoA likely plays a non-cell autonomous role during development. The localization of wild type and mutant cells in the fruiting body structure was determined by staining with X-Gal solution. Wild type cells expressing β-galactosidase, known as HR30 cells, stain blue and can be identified in the fruiting body. The localization of RnoA OE cells is inferred by identifying the unstained cells. RnoA OE cells localize to the stalk of the fruiting body structure, while HR30 cells localize to the spore mass. The predominance of RnoA OE cells in the stalk suggests these mutants undergo cell sorting or differentiation differently than wild type cells. Specifically, RnoA OE cells may be deficient in prespore cell differentiation since RnoA OE cells preferentially sort to the stalk in chimeric mixtures with wild type cells. This implies that RnoA may potentially play a role in the differentiation or sorting of prespore cells during development.

In *D. discoideum* development, mound formation occurs after the aggregation of starved cells. In this developmental stage, cells begin to organize and sort into distinct populations that

will dictate their ultimate localization in the fruiting body. The formation of the mound is a complex process involving cell differentiation, cell sorting, chemotaxis, and adhesion, processes rooted in effective organization of the actin cytoskeleton (41). During the process of mound formation, the uniform population of aggregated cells begins to differentiate into prespore and prestalk cell types (34) (1) (95). In addition to its role in cell aggregation, cAMP chemotaxis also drives mound formation through the spatial organization of different cell types, a process known as cell sorting (90) (74). As prestalk cells are best able to respond to cAMP and exhibit greater chemotactic motility than prespore cells, prestalk cells migrate toward the mound center and then sort to the top of the mound, forming the organizing center known as the tip (90) (54). The cells in the organizing tip coordinate an effective and synchronized response to cAMP to facilitate development beyond the mound stage (95) (19). The prespore cells are less responsive to cAMP and therefore lag behind the prestalk cells.

In this light, the developmental defects of the RnoA mutant cells may be the result of a defective cAMP response. The overproduction of RnoA may interfere with effective cAMP chemotaxis and thus prevent proper formation of an organizing tip, halting development past the mound stage. The developmental delay of the RnoA antisense cells, caused by a prolonged aggregation stage, may potentially be due to decreased or ineffective cAMP chemotaxis due to reduced RnoA in these cells. As the RnoA antisense cells do eventually form fruiting bodies, decreased RnoA expression does not impair these mutants from responding to cAMP after the mound stage of development. The observed decrease in endogenous RnoA levels after the mound stage further supports the idea of RnoA not being required for cAMP chemotaxis during later stages of development.

In addition to chemotactic properties, mechanical interactions such as cell-cell contacts and cell-substrate adhesion play a crucial role in development, particularly in the transition from aggregate to mound (39). As cells chemotax to aggregate, several cell-surface adhesion molecules are expressed and have distinctive roles throughout development. For example, the cell adhesion molecule gp80 is present at sites of cell-cell contact from aggregation through the mound and slug stages of development, where it stabilizes cell adhesion as well as regulates aggregate size (84). The *lagC* gene, which encodes the cell adhesion glycoprotein gp150, is essential for progression beyond late aggregation through its involvement in cell sorting and morphogenesis (94) (83). Cells lacking *lagC* exhibit a perpetual pattern of aggregation and disaggregation, implying cell cohesion plays a role in maintaining the integrity of the aggregate (21). As prestalk and prespore cells migrate within the mound, cell-cell contacts are continuously made and broken. This adhesion is known to influence cell sorting in the mound, as well as in the slug. Differences in cell adhesion between prespore and prestalk cell types promotes cell sorting by favoring adhesion to the same cell type, enabling distinct spatial localization of prespore and prestalk cells (62).

Given the prominence of cell cohesion in multicellular development, the mound stage arrest of the RnoA OE cells and the developmental delay of the RnoA antisense cells may be the result of defective cell-cell contacts. Defects in cellular adhesion may interfere with proper cell sorting, leading to the mound arrest phenotype observed in the RnoA OE cells. Alterations in cell adhesiveness can also affect cell motility, thus the developmental delay of the RnoA antisense cells could potentially be due to abnormal cell-cell cohesion interfering with cell motility during the aggregation stage.

As its mammalian homolog activates reorganization of the actin cytoskeleton, RnoA may potentially influence *D. discoideum* development through the regulation of the actin cytoskeleton. Many of the physiological processes which occur during development, such as chemotaxis and cell adhesion, are dependent upon regulated alterations to the cytoskeleton. Thus, RnoA may organize the actin cytoskeleton to ensure actin dependent processes appropriately transpire during development. The observed developmental defects in the RnoA mutant cells may therefore be the result of impairments in actin-dependent processes such as chemotaxis or cellular adhesion. To address these possibilities, the chemotactic and adhesive properties of the RnoA mutant cells will be explored in the following chapters.

CHAPTER 4: RnoA mediates cAMP signals to organize actin

4.1 RnoA mutants fail to stream.

As starving cells become responsive to cAMP, they become polarized and chemotax toward the aggregation center in a head-to-tail manner known as streaming (45). These streams of chemotaxing cells give rise to aggregates. To better understand the developmental defects associated with RnoA misexpression, the process of aggregation was examined in more detail. Wild type and RnoA mutant cells were allowed to aggregate at low cell density in submerged culture. Wild type cells undergo streaming to form aggregates at 56 x 10^3 cells/cm^2 (**Figure 10**). In contrast, both RnoA OE and RnoA antisense cells fail to stream and only form few aggregates, even at high cell concentrations. Thus, proper RnoA expression appears to be required for effective cell streaming and aggregation.

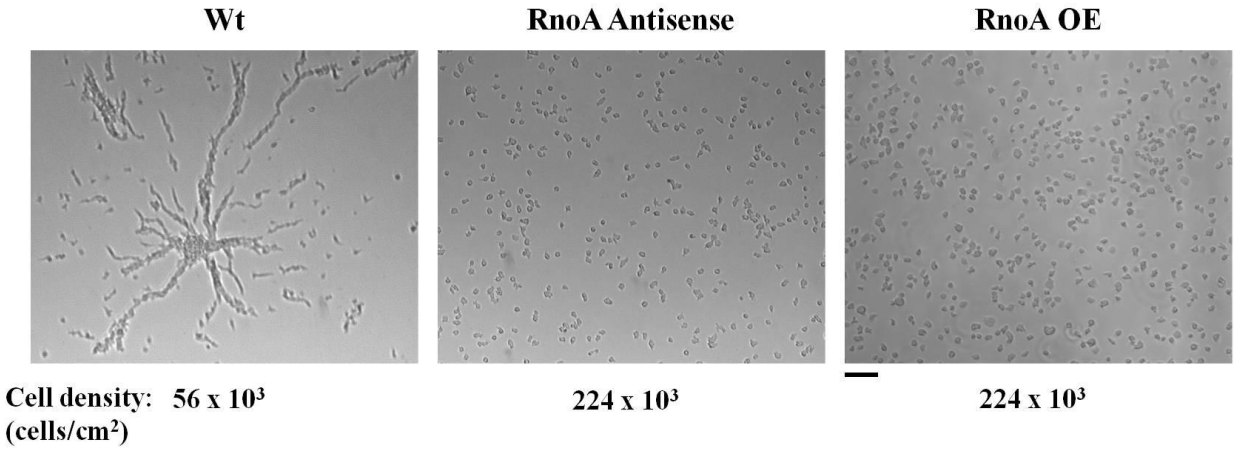

Figure 10: RnoA mutant cells do not undergo cell streaming. Wild type and RnoA mutant cells were starved for 16 hrs under PBM at varying low cell densities. Bar, 1 mm.

4.2 RnoA is involved in cAMP chemotaxis.

Cell streaming during aggregation is due in part to efficient chemotaxis to cAMP. Given the absence of cell streaming in the RnoA mutants, it is possible these cells have flawed chemotaxis. To determine whether RnoA plays a role in cAMP chemotaxis, under-agarose chemotaxis assays were performed. In these assays, the ability of cells to efficiently migrate out of a trough and under agarose toward a chemoattractant is determined. Chemotaxis is defined by the speed, directionality, and chemotactic index of a cell. Directionality is a measure of a cell's ability to travel on a straight path. It is calculated as (absolute distance traveled)/ (total path length), where a maximum value of 1 represents a straight path without deviations and a value of 0 represents a random walk. The chemotactic index is a measure of a cell's ability to sense and respond to a chemotactic gradient. It is determined by calculating the cos θ, where θ represents the angle of deviation between a straight line up the chemotactic gradient and the net path of a cell. A value of 1 is equivalent to a path up the chemotactic gradient. A value of 0 represents movement perpendicular to the gradient. A value of -1 represents movement down the gradient. Wild type, RnoA OE, and RnoA antisense cells were starved for 5 hrs and then assessed for chemotaxis toward cAMP (**Table 1**). Consistent with previous findings (57) (31) , wild type cells crawl under the agarose and migrate toward increasing cAMP concentrations, with a speed of 10.20 ± 0.49 μm/min, a directionality of 0.79 ± 0.05, and a chemotactic index of 0.94 ± 0.02. Unlike the wild type cells, RnoA OE and RnoA antisense cells do not travel under the agarose toward higher concentrations of cAMP. Instead, they remain in the trough, suggesting that they are unable to chemotax toward cAMP. This argues a role for RnoA in chemotaxis toward cAMP.

cAMP Chemotaxis			
	Wt	**RnoA antisense**	**RnoA OE**
Speed (μm/min)	10.20 ± 2.45	N/A	N/A
Directionality	0.79± 0.05	N/A	N/A
Chemotactic Index	0.94 ± 0.01	N/A	N/A

Table 1: cAMP chemotaxis of wild type and RnoA mutant cells. Wild type and RnoA mutant cells were starved for 5 hrs on filter pads and harvested. Time-lapse images of cells migrating under agarose toward 10 μM cAMP were then taken. Individual cells were tracked with ImageJ software. Directionality is defined as net distance / total path. The chemotactic index is calculated as the cos θ, where θ is the angle of deviation between a direct line up the chemical gradient and the net path of a cell. Values represent the mean of >3 experiments ± SEM.

4.3 RnoA does not play a role in folate chemotaxis.

The observed defect in cAMP chemotaxis of the RnoA mutants could be due to a general defect in chemotaxis. To address this possibility, we examined the cells' ability to chemotax to folate using the same assay. Vegetative *D. discoideum* cells chemotax toward folate as a means of tracking bacterial prey (63). Cells lose sensitivity to folate after seven to nine hours of starvation and instead become responsive to cAMP secreted by other starving cells (41) (101). While folate chemotaxis and cAMP chemotaxis have been shown to utilize distinct cell-surface receptors and signaling pathways (101) (67), the underlying mechanics of cell motility remain the same. Wild type cells chemotax to folic acid with a speed of 11.29 ± 0.71 μm/min, a directionality of 0.61 ± 0.03, and a chemotactic index of 0.78 ± 0.04. Similar to wild type cells, RnoA antisense cells have a speed of 12.18 ± 0.44 μm/min, a directionality of 0.72 ± 0.04, and a chemotactic index of 0.84 ± 0.04, while RnoA OE cells have a speed of 12.39 ± 1.09 μm/min, a directionality of 0.64 ± 0.04, and a chemotactic index of 0.71 ± 0.04 (**Figure 11)**. The values for both mutants are not significantly different from those of the wild type cells ($p > 0.05$). This

suggests that RnoA is not involved in chemotaxis to folate, but is specifically involved in cAMP chemotaxis.

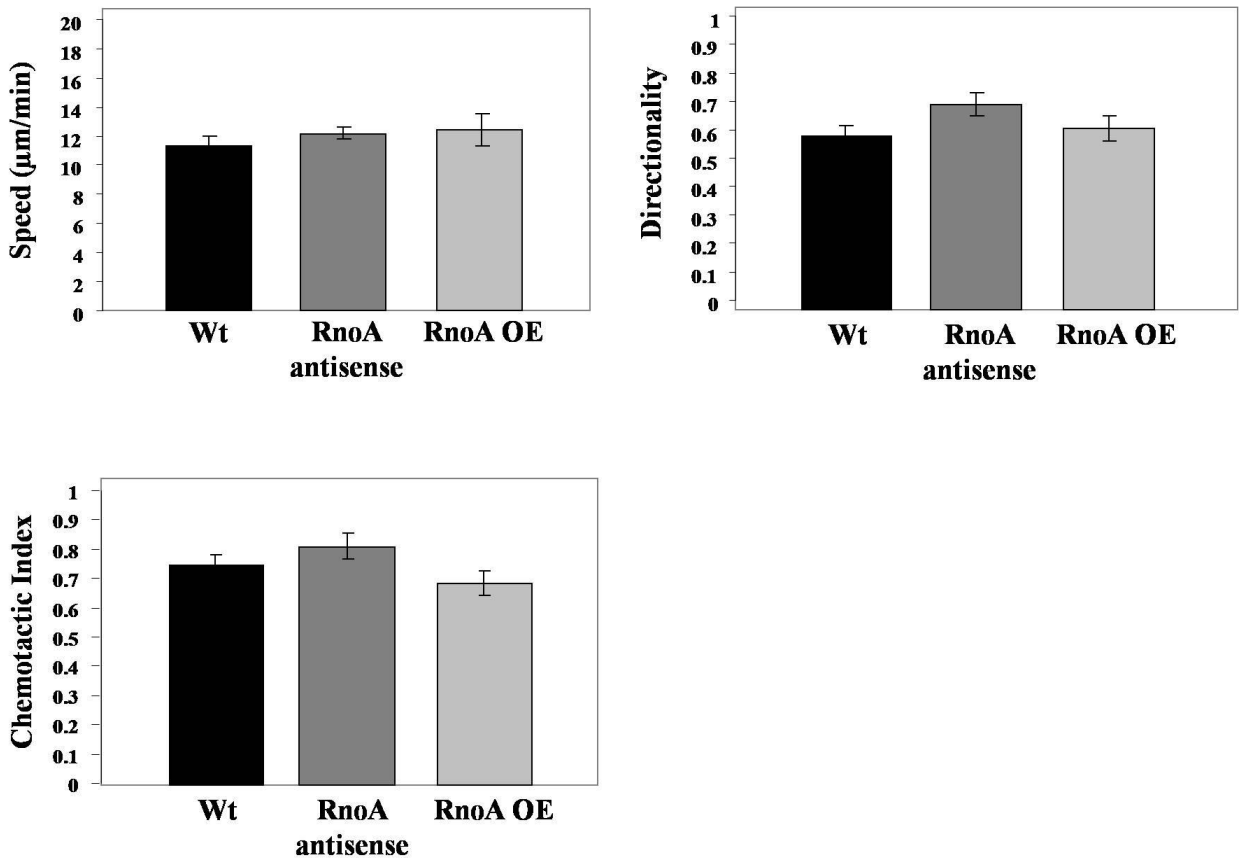

Figure 11: RnoA mutants undergo chemotaxis to folate. Time-lapse images of vegetative cells migrating under agarose toward 1 mM folate were taken. Individual cells were tracked with ImageJ software. Directionality is defined as net distance / total path. The chemotactic index is calculated as the cos θ, where θ is the angle of deviation between a direct line up the chemical gradient and the net path of a cell. Values represent the mean of >5 experiments ± SEM.

4.4 RnoA mutants are not defective in cell motility.

An inability to chemotax toward cAMP could be due to defective cell motility in starved cells or the inability to sense the presence of the chemoattractant. To distinguish between these two possibilities, the motility of wild type, RnoA OE, and RnoA antisense cells in the absence

and presence of cAMP was determined. Wild type cells have been shown to exhibit a change in cellular speed in the presence of cAMP, a property termed chemokinesis (86) (14). Cells were starved for 6 hours in submerged cultures then random motility was measured both before and after global stimulation with 5 µM cAMP. In the absence of cAMP, wild type cells have a speed of 9.23 ± 0.31 µm/min. Both RnoA OE and RnoA antisense cells exhibit similar speeds of 9.59 ± 0.65 and 10.43 ± 0.41 µm/min, respectively, indicating that these cells do not have defective motility under starvation conditions (**Figure 12A**). However, in the presence of cAMP (**Figure 12B**), while wild type cells have drastically reduced their speed (5.77 ± 0.19 µm/min), RnoA antisense and RnoA OE cells have only slightly decreased cell speeds (7.03 ± 0.45 and 7.92 ± 0.28 µm/min, respectively). This suggests that the RnoA mutant cells respond differently to cAMP than wild type cells.

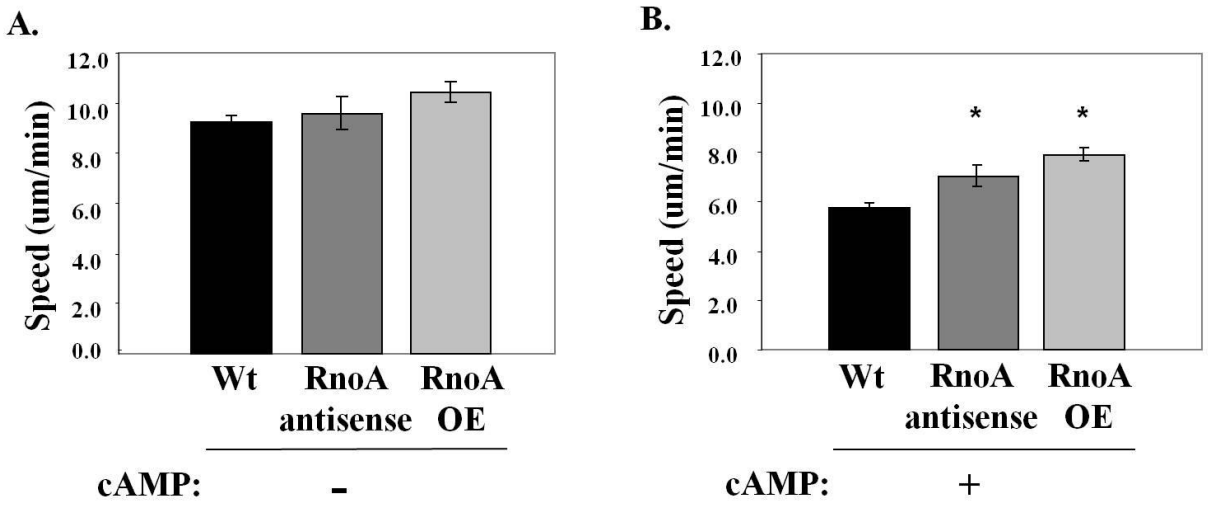

Figure 12: RnoA mutants have altered cell motility in presence of cAMP. Cells were starved for 6 hrs under PBM. Time-lapse images were taken before (A) and after (B) global stimulation with 5 µM cAMP. Individual cell were tracked with ImageJ software. Values represent the mean of >3 experiments ± SEM. *, P < 0.01 compared with wild type control (Student's t test).

4.5 RnoA plays a role in cell polarization in response to cAMP

In the presence of a cAMP gradient, chemotaxing cells become polarized along the gradient. This polarization is established by polymerizing F-actin at the leading edge of the cell, in the direction of the cAMP source, while recruiting various intracellular signaling molecules to distinct locations in the cell (43) (93). The creation of cell polarity is critical for a cell to effectively move up a chemotactic gradient. Since cell polarity depends upon the organization and regulation of the actin cytoskeleton, deficiencies in this organization can result in an impaired chemotactic response. As RnoA antisense cells and RnoA OE cells do not chemotax toward cAMP, these cells may not properly polarize in response to a cAMP gradient. To address this, 5 hr starved wild type cells, RnoA antisense cells, and RnoA OE cells were placed in a gradient of cAMP containing a maximum concentration of 10 μM mixed with 20 mg /ml FITC-Dextran. The presence of the gradient was confirmed by visualizing the diffusion of FITC-Dextran. After allowing time for the cells to sense the gradient, the cells were fixed and stained for F-actin. Cell polarity was quantified by calculating the ratio of the minor axis to the major axis of individual cells. A value of 1 indicates a cell is a perfect circle and is not polarized. As a cell becomes more polarized, it becomes more elliptical, and therefore the value decreases. As seen in **Figure 13**, wild type cells effectively polarize along the gradient, exhibiting an elongated phenotype with a circularity of 0.671 ± 0.020. RnoA antisense cells, however, appear very round and have a circularity of 0.783 ± 0.024. RnoA OE cells are also less polar then the wild type cells with a circularity of 0.812 ± 0.012. Taken together, this suggests a role for RnoA in cell polarity in response to a cAMP gradient.

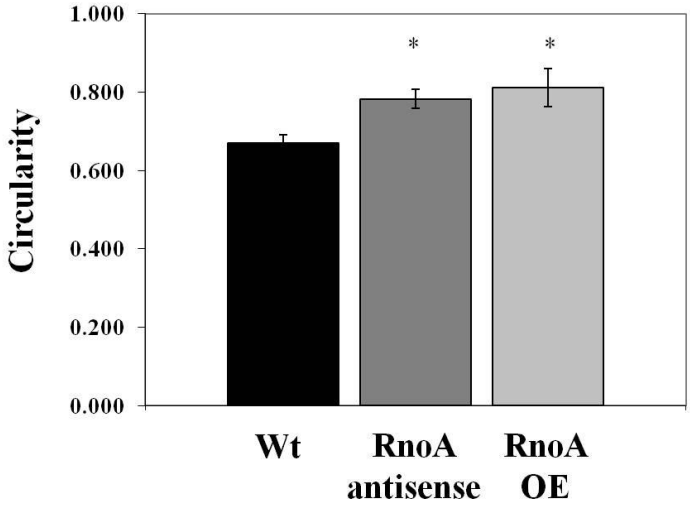

Figure 13: RnoA mutants have polarity defects in cAMP gradient. Cells were starved for 5 hrs then placed in a cAMP gradient with a maximum concentration of 10 μM. Cells were fixed and stained with Rhodamine-Phalloidin to visualize F-actin organization. Cell polarity was quantified with Image J software and measured as the ratio of a cell's minor axis to its major axis. Values represent the mean of >3 experiments, each examining at least 40 cells ± SEM. *, $P < 0.08$ compared with wild type control (Student's t test).

4.6 RnoA is involved in F-actin polymerization in response to cAMP

Exposure of a cell to a chemoattractant initiates the reorganization of the actin cytoskeleton to allow for the appropriate chemotactic response. In response to cAMP, *D. discoideum* cells exhibit two distinct phases of actin polymerization. The first phase consists of a rapid increase in F-actin polymerization approximately 5 seconds after stimulation followed by a prompt return to basal levels of polymerization within 30 seconds (11). The second phase, a more modest but stable increase in polymerization, occurs approximately 60 seconds after stimulation and is correlated to pseudopod extension (11) (97). This second F-actin polymerization peak is thought to play a role in optimizing the chemotactic response as its distruption has been shown to result in poor chemotaxis (97). As the RnoA antisense cells and

the RnoA OE cells fail to undergo cAMP chemotaxis and given that F-actin polymerization is involved in chemotaxis, these mutants may be deficient in F-actin polymerization. To explore this possibility, the ability of RnoA mutant cells to polymerize F-actin in response to cAMP was examined. Wild type cells, RnoA antisense cells, and RnoA OE cells were starved for 5 hours then stimulated with 1 μM cAMP. Samples were then collected at various time points up to 150 seconds after stimulation and immediately fixed and incubated in a buffer containing AlexaFluor Phalloidin, an F-actin binding fluorescent probe. The fluorescence of each sample was then measured with a plate reader.

As reported in the literature, cAMP stimulates a sharp 1.6-fold increase in F-actin polymerization in wild type cells (—◆—) after 5 seconds and a smaller, broader peak 60 seconds after stimulation (**Figure 14A**). RnoA antisense cells (—■—) also have a rapid increase in polymerization (approximately 1.5-fold) 5 seconds after cAMP stimulation. Unlike wild type cells which return to basal levels of F-actin polymerization by 30 seconds, the RnoA antisense cells maintain an elevated level of F-actin polymerization which gradually decreases to 1.3-fold of the basal value by 60 seconds. A second broad peak of lower intensity is observed in the RnoA antisense cells between 80 and 100 seconds after stimulation. This second peak of polymerization occurs later than in wild type cells and has a higher intensity than in the wild type cells. RnoA OE cells (---▲---) also display an increase in F-actin polymerization 5 seconds after cAMP stimulation, though the increase is smaller than that of wild type cells. F-actin polymerization levels quickly return to basal levels by 20 seconds after stimulation, sooner than in wild type cells. 30 seconds after stimulation, when wild type cells have basal levels of polymerization, RnoA OE cells display a second peak of F-actin polymerization that persists until approximately 80 seconds after stimulation. As compared to wild type cells, the pattern of

F-actin polymerization in response to cAMP stimulation is distinctly altered in the RnoA mutant cells.

To test if the variations in F-actin polymerization of the RnoA mutants are specific to cAMP stimulation, the ability of vegetative wild type cells, RnoA antisense cells, and RnoA OE cells to polymerize F-actin in response to folate was analyzed. As depicted in **Figure 14B**, 5 seconds after stimulation with 50 μM folate, wild type cells, RnoA antisense cells, and RnoA OE cells all display a sharp peak of F-actin polymerization between 1.3-fold and 1.6-fold that of basal levels. As the RnoA mutants are able to polymerize F-actin to the same level as wild type cells in response to folate, the defects observed in F-actin polymerization after cAMP stimulation are specific to cAMP.

A.

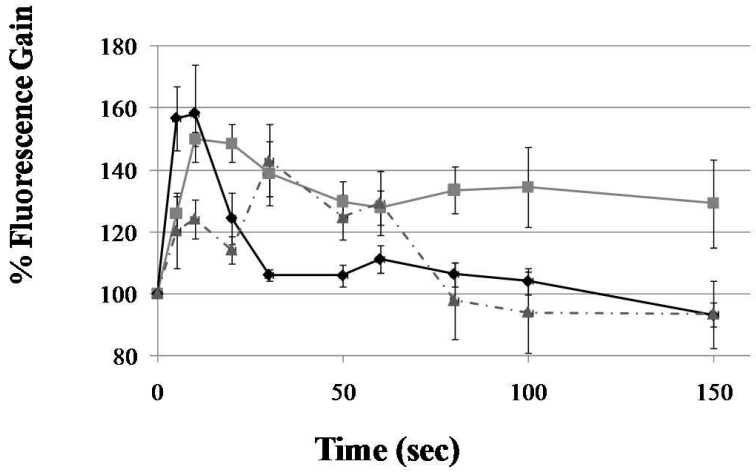

B.

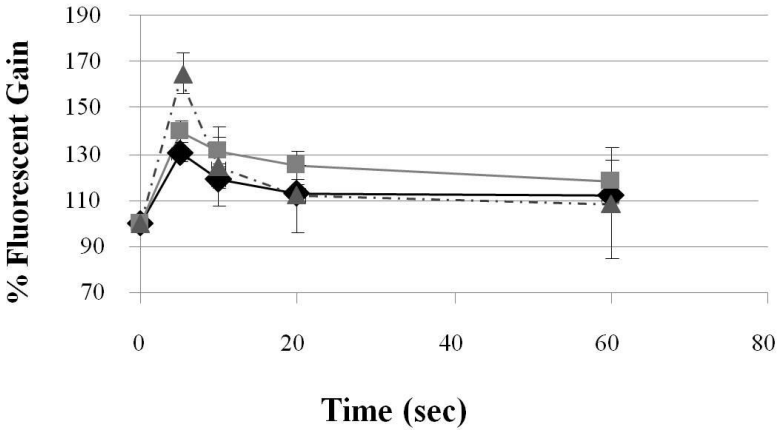

Figure 14: RnoA mutants polymerize F-actin differently than wild type cells. F-actin polymerization was quantified by measuring the level of Phalloidin in samples of wild type (—◆—), RnoA antisense (—■—), and RnoA OE (- -▲- -) cells taken at various time points after stimulation by (A) 1 µM cAMP or (B) 50 µM folate.

4.7 Proper RnoA expression is needed for actin organization.

Chemotaxis is a multi-faceted process that requires a cell to detect the chemoattractant gradient and polarize along the gradient before migration toward the chemoattractant source can ensue (2) (89). As these processes are heavily dependent upon the actin cytoskeleton, defects in F-actin organization can lead to impaired cell polarity and chemotaxis. Given the defects in

cAMP stimulated F-actin polymerization, the RnoA antisense cells and the RnoA OE cells may have abnormalities in the organization of F-actin. To ascertain whether F-actin distribution is dependent upon RnoA, F-actin was visualized in wild type and both RnoA mutant cells using Rhodamine Phalloidin. As seen in **Figure 15A**, 6 hr starved wild type cells have F-actin distributed in filopodia and broad membrane protrusions. RnoA antisense cells have similar F-actin organization compared to wild type cells, indicating that RnoA decreased to these levels of expression does not detectably alter F-actin organization within the cell. However, RnoA OE cells display an increased number of filopodia compared to wild type cells and have bright spots of cytosolic F-actin. To determine whether the overall amount of F-actin is altered by a change in RnoA levels, the average mean intensity per cell for the RnoA mutant cells was compared to that of wild type cells. As depicted in **Figure 15B**, the average mean intensity per cell of the RnoA antisense cells was calculated as 100% ± 17% of the wild type cells, while RnoA OE cells were 95% ± 9% of the wild type mean intensity. As wild type cells and both RnoA mutants have a similar mean intensity per cell, RnoA antisense cells and RnoA OE cells likely have similar levels of F-actin compared to wild type cells. Taken together, the data suggest that a reduction of RnoA expression does not significantly alter F-actin organization, but the overexpression of RnoA does cause distinct changes in F-actin localization compared to wild type cells, without significantly changing the overall levels of polymerized actin.

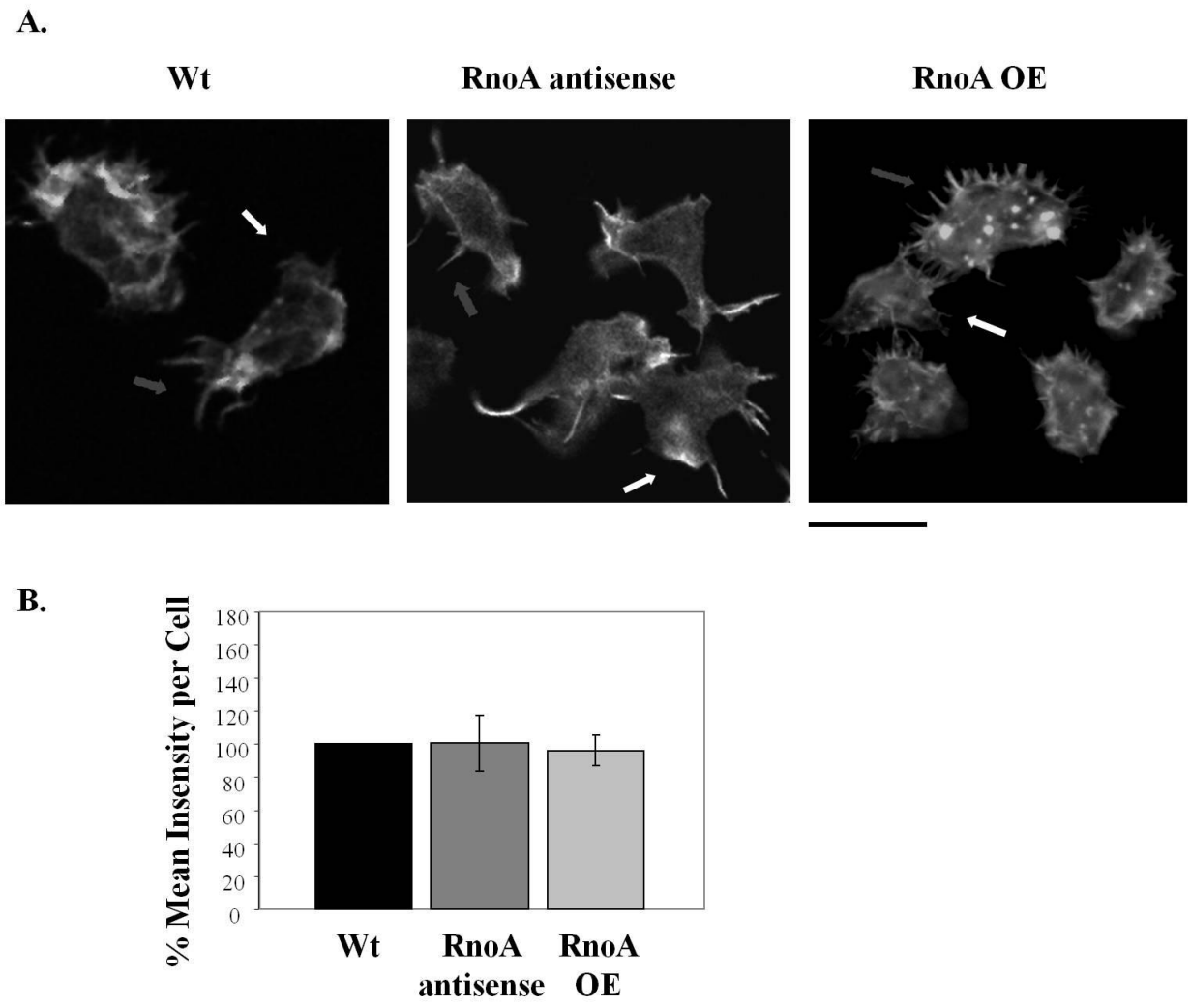

Figure 15: Actin organization is altered in RnoA mutant cells. (A) Cells were starved for 6 hrs before fixation. Cells were stained with Rhodamine-Phalloidin to visualize F-actin organization. White arrows indicate sites of membrane protrusions. Gray arrows indicate filopodia. Bar, 10 μm. (B) The mean intensity of Rhodamine-Phalloidin per cell was quantified with Image J software. Values represent the mean of at least 10 cells ± SEM.

4.8 Discussion.

In the previous chapter, we demonstrated how RnoA is involved in mound formation and differentiation. In this chapter, to complement these findings and to explore the role of RnoA in development, we analyzed cell streaming, one of the processes involved in mound formation. During development, cells form aggregates by undergoing cell streaming, a process where

individual, polarized cells form head-to-tail interactions as they chemotax toward the chemoattractant source. The development of undersized fruiting bodies by the RnoA antisense cells may originate from defects in cell streaming. During low density aggregation assays, RnoA antisense cells remain as single cells, failing to form streams. RnoA antisense cells thus form significantly smaller agglomerates compared to wild type cells, as they are not able to recruit the majority of cells into aggregates. As aggregates were only detected at the highest densities tested, it is likely that RnoA antisense cells merely adhere to neighboring cells at higher densities. Therefore, the aggregation observed in RnoA antisense cells plated onto filter pads may not be due to cell streaming, but rather the result of cell-cell cohesion in a population of densely packed cells, generating small mounds. RnoA antisense cells may therefore produce smaller sized fruiting bodies due to the small mounds formed by cell adhesion to neighboring cells, rather than through cell streaming. The prolonged aggregation and mound formation observed in the RnoA antisense cells is therefore a result of inefficient random cell adhesion generating small mounds instead of cAMP-directed cell streaming seen in wild type cells.

Given that the process of cell streaming is partly driven by effective cAMP chemotaxis, the inability of the RnoA antisense cells to stream may therefore be due to defects in cAMP chemotaxis. As cAMP chemotaxis is a fundamental process in development, particularly in the transition from single cells to multicellular structures, the ability of RnoA mutants to undergo chemotaxis was tested. RnoA OE cells and RnoA antisense cells both fail to chemotax toward cAMP, as indicated by under agarose chemotaxis assays. The observed chemotactic defect is specific to cAMP mediated chemotaxis as the RnoA mutants in the vegetative state undergo chemotaxis to folate without impairment. Furthermore, the observed failure of RnoA antisense and RnoA OE cells to chemotax toward cAMP is not a result of defective cell motility. RnoA

mutant cells exhibit similar cell speed compared to wild type cells in the absence of cAMP, suggesting that the RnoA antisense and RnoA OE cells do not have deficiencies in cell motility. In the presence of cAMP, however, both RnoA mutants fail to have a decrease in speed as is observed in wild type cells. This finding suggests that cell motility in RnoA antisense and RnoA OE cells is not impaired, but rather these cells do not properly respond to cAMP as compared to wild type cells. The inability of the RnoA mutant cells to chemotax to cAMP is therefore likely due to a faulty cAMP signaling cascade as these cells display cell motility comparable to wild type cells in the absence of cAMP and significantly altered cell speed after addition of cAMP. Coupled with the finding that the RnoA mutants chemotax to folate, the data suggest RnoA antisense and RnoA OE cells are not defective in general chemotaxis or motility, but rather are deficient in responding to cAMP, which leads to impaired cAMP chemotaxis.

The chemotactic impairment of the RnoA antisense cells may be the underlying cause of the developmental defects in these cells. The inability of the RnoA antisense cells to undergo cell streaming during the aggregation stage of development may be due to flawed chemotaxis, as cell streaming is dependent upon efficient chemotaxis toward cAMP. Defects in cAMP chemotaxis may interfere with normal cell streaming during aggregation, delaying the aggregation process and extending the total time needed to complete development. This phenomenon has been observed in other *D. discoideum* mutants such as cells lacking LrrA, a leucine-rich repeat protein involved in morphogenesis. *lrrA*$^-$ cells are able to form mounds, but are unresponsive to a cAMP gradient and fail to undergo streaming (50). As the remainder of development proceeds with normal timing after aggregation occurs, the developmental delay of the RnoA antisense cells may be due to improper cAMP chemotaxis only during aggregation.

RnoA may therefore not play a prominent role in cAMP chemotaxis during later stages of development, when RnoA expression is minimal.

The developmental arrest of the RnoA OE cells may also be the result of faulty cAMP chemotaxis. Like the RnoA antisense cells, RnoA OE cells do not undergo chemotaxis or form streams during low cell density assays. RnoA OE cells likely adhere to neighboring cells at high cell densities to form a mound rather than aggregating through chemotaxis. As described earlier, the process of mound differentiation and cell-type sorting is largely dependent upon cAMP chemotactic signaling. Differentiated prestalk cells respond to cAMP waves by sorting to the mound tip, where they lead development beyond the mound stage. As the RnoA OE cells do not chemotax toward cAMP, formation of an organizing center is likely impaired. In addition, proper sorting of prestalk and prespore cells may be hindered as cell sorting is strongly influenced by the chemotactic properties of these cell types. Without the leadership of an organizing center, the RnoA OE cells are unable to progress beyond the mound stage. As RnoA antisense cells ultimately form fruiting bodies, these mutants are likely able to establish an organizing center. Given the prolonged aggregation and mound formation, these cells may require more time to generate an organizing tip. As demonstrated by cAMP chemotaxis assays, manipulating RnoA expression blocks the ability of a cell to properly respond to cAMP, thereby preventing chemotaxis and possibly streaming, implying that RnoA is involved in the chemotactic response to cAMP. Consistent with its protein expression pattern, RnoA appears to be involved in the cAMP response during aggregation when peak expression occurs, but does not seem to play a significant role further into development when RnoA expression is low.

Directional cell movement is a multifaceted process involving the detection of the chemoattractant gradient, establishment of a leading edge, and cell polarization to generate

forward cell movement (2) (89). RnoA antisense cells and RnoA OE cells appear to be defective in their ability to sense the chemoattractant gradient as these cells did not exhibit the characteristic change in speed in the presence of cAMP. A cell also polarizes along the chemoattract gradient prior to chemotactic movement, changing from a spherical shape to an elliptical shape. RnoA antisense cells and RnoA cells are both significantly less polar than wild type cells in the presence of a cAMP gradient, again suggesting a defect in sensing and responding to cAMP. During chemotaxis, F-actin is polymerized along the chemotactic gradient at the leading edge and is correlated to pseudopod formation (43) (2). The polymerization of F-actin in discrete regions within the cell drives cell polarity and enables pseudopod extension at the leading edge of a cell and therefore migration toward the chemoattractant. Defects in cell polarity are often due to defeciences in F-actin polymerization and can impair the chemotactic response. As the RnoA mutants do not display appropriate cell speed or cell polarity in response to cAMP, suggesting these cells either do not sense the chemoattractant or cannot respond to the chemical signal, the ability of RnoA antisense cells and RnoA OE cells to polymerize F-actin in response to cAMP stimulation was assessed. While the initial spike in F-actin polymerization as a result of cAMP in both RnoA antisense cells and RnoA OE cells occurs with the same timing and intensity as in wild type cells, the continuing pattern of polymerization is vastly different. RnoA antisense cells experience a prolonged increase in F-actin polymerization until 60 seconds after stimulation whereas wild type cells return to basal levels of polymerization by 30 seconds. The second F-actin polymerization peak is delayed in the RnoA antisense cells and the levels of polymerization are elevated beyond that of wild type cells. The RnoA OE cells, on the other hand, readily return to basal levels of F-actin polymerization by 20 seconds, much sooner than the wild type cells. The second polymerization peak also occurs earlier in the RnoA OE cells, 30

seconds after cAMP stimulation, instead of after 60 seconds as observed in wild type cells. The alteration of F-actin polymerization in the RnoA mutants as compared to wild type cells suggests that both RnoA antisense cells and RnoA OE cells deviate from the typical timing of F-actin polymerization in response to cAMP. The defects in F-actin polymerization of the RnoA mutants are specific to cAMP as RnoA antisense cells and RnoA OE cells follow the same pattern of F-actin polymerization as wild type cells in response to folate stimulation. Therefore, RnoA may be involved in regulating the timing of F-actin polymerization in response to cAMP as the loss of RnoA delays polymerization and RnoA over production leads to premature polymerization. The second peak of F-actin polymerization, which occurs 60 seconds after cAMP stimulation in wild type cells, is associated with pseudopod extension (11). Given that the both the timing and intensity of this second F-actin polymerization peak in the RnoA mutant cells differs from that of wild type cells, RnoA antisense cells and RnoA OE may have altered pseudopod formation, which can interfere with proper chemotaxis. Given the failure of the RnoA mutants to respond to global stimulation of cAMP, the lack of cell polarity in a cAMP gradient, and the distorted pattern of F-actin polymerization after cAMP stimulation, RnoA antisense cells and RnoA OE cells do not effectively respond to cAMP. Therefore, RnoA appears to be important for a cell to appropriately sense and respond to cAMP in order to polarize, polymerize actin, and ultimately undergo chemotaxis. Defects in the cAMP signaling pathway may be the source of the chemotactic impairments in the RnoA mutants.

As the proper organization of polymerized F-actin is an important component of directed cell movement, disruption of this organization can result in chemotactic defects. Given the inability of the RnoA mutants to chemotax toward cAMP, coupled with the observed polarity and F-actin polymerization defects, the distribution of F-actin in starved RnoA antisense cells

and RnoA OE cells was examined. The reduced levels of RnoA present in the RnoA antisense cells appear to be sufficient to organize F-actin, as the distribution of F-actin was comparable to that of wild type cells. However, as Phalloidin staining only provides a gross picture of F-actin distribution, variations in the types of F-actin networks formed can not be distinguished. Alterations in these networks may potentially prevent the proper F-actin organization required for cAMP chemotaxis to occur. While we did not detect altered F-actin organization in cells with reduced RnoA levels, we did observe an increased number of filopodia compared to wild type cells and bright spots of cytosolic F-actin when RnoA was over produced. This may potentially be due to improper localization of RnoA caused by elevated RnoA production. As F-actin is localized to the cell periphery, particularly the leading edge, during chemotaxis, it is possible that the mislocalization of F-actin to the cytosol may impede the chemotactic ability of the RnoA OE cells. In addition, the excessive filopodia present in the RnoA OE cells, coupled with altered F-actin polymerization, may impair effective movement up the chemotactic gradient. Taken together, these findings are consistent with RnoA being an upstream regulator of F-actin organization, like its mammalian homolog (26).

A wide variety of proteins serve as upstream regulators of F-actin organization. Members of the Ras superfamily of small guanine nucleotide triphosphatases (GTPases), such as Ras, Rho, and Rac, are known to organize the actin cytoskeleton through various signal transduction pathways in response to activation of cell surface receptors (29) (78). GTPases are in turn regulated by guanine nucleotide exchange factors (GEFs), which enable GTPase activity. Several *D. discoideum* Ras and Rac GEFs have been associated with actin cytoskeletal organization. The loss of any of these GEFs prevents cell streaming and delays development (2) (96) (55). As RnoA has sequence similarity to GEFs, and cells misexpressing RnoA have

defective cAMP chemotaxis and actin organization, RnoA likely serves as a GEF for an undetermined Arf family protein in order to coordinate chemotactic signals and cytoskeletal rearrangements.

The defeciences of the RnoA OE cells are therefore likely due to impairments in the signaling pathways that govern chemotactic response and actin cytoskeletal rearrangements. The RnoA OE cells arrest at the mound stage of development, likely due to the inability to form the organizing tip which leads development past the mound stage. These mutants fail to form the organizing tip as the cells are unable to chemotax in response to cAMP. cAMP chemotaxis requires cells to effectively sense the chemoattractant and polarize along the chemoattractant gradient. RnoA OE cells do not undergo cAMP chemotaxis as they cannot properly polarize along a cAMP gradient. Cell polarity is likely impaired due to the improper timing of F-actin polymerization in the RnoA OE cells. The altered pattern of F-actin polymerization may be the source of the multiple pseudopods observed in the RnoA OE cells.

The RnoA antisense mutants also exhibit developmental defects. RnoA antisense cells are significantly delayed in development due to a prolonged aggregate stage. The extended aggregation stage is likely caused by the inability of the RnoA antisense cells to undergo cell streaming. The cell streaming defect of these mutants is also likely due to the failure to properly chemotax toward cAMP. Like the RnoA OE cells, the RnoA antisense cells do not undergo cAMP chemotaxis, most likely as a result of poor cell polarity and improper F-actin polymerization.

Given the characteristics of the RnoA antisense cells and the RnoA OE cells, RnoA appears to be intimately linked to the coordination of cAMP chemotactic signals with F-actin organization, specifically the polymerization of F-actin in response to cAMP. As evidenced by

the RnoA antisense and RnoA OE mutant cells, alteration of RnoA basal levels modifies the pattern of F-actin polymerization. Consquently, F-actin may not be properly localized within the cell and the ability of a cell to effectively polarize in response to cAMP and undergo cAMP chemotaxis is greatly impaired, thereby delaying or halting development. To gain more insight regarding the role of RnoA in actin organization, the potential protein interaction partners of RnoA will be examined in the following chapter. In addition, the role of such interactions in actin-dependent processes will also be explored.

CHAPTER 5: RnoA forms a complex with PldB and PaxB

5.1 ARNO interactions.

Given the participation of mammalian ARNO in many actin-dependent processes, ARNO may interact with many proteins from various signaling pathways. Two potential interaction partners for ARNO include the enzyme phospholipase D (PLD), which produces phosphatidic acid (27), and the adaptor protein paxillin, a key player in adhesion. ARNO, PLD, and paxillin have all been functionally linked to the actin cytoskeleton and are involved in actin mediated processes. These three proteins colocalize to areas of active actin remodeling such as lamellipodia and membrane ruffles (64) (68) (70). ARNO may participate in the localization of paxillin as Arf6, the downstream target of ARNO, mediates localization of paxillin to focal adhesion sites (44). In addition, the PLD1 isoform of PLD partially colocalizes with paxillin in focal adhesion sites (35). ARNO may also serve to regulate PLD as evidence suggests ARNO promotes PLD activation during actin dependent processes such as cell migration (70). PLD activity has been found in cell membrane fractions containing regulatory proteins such as Arfs, the downstream targets of ARNO, and paxillin (36). The functional association of ARNO, PLD, and paxillin to the actin cytoskeleton and its mediated processes promotes the possibility of a protein complex containing catalytic PLD properties, regulatory proteins such as Arfs and ARNO, and adaptor proteins such as paxillin (36). Such a complex may play a role in the coordination and regulation of actin cytoskeletal organization required for processes such as adhesion and motility.

The relationship between ARNO, PLD, and paxillin can be explored in *Dictyostelium discoideum* as this organism carries homologs for these proteins: RnoA, PldB, and PaxB,

respectively. PldB and PaxB have peak expression between 12 and 16 hours into development (12) (8), approximately when RnoA has peak expression. In addition, PldB and PaxB, like their mammalian counterparts, are also known to mediate actin-related processes. PLD activity in *D. discoideum* plays a role in cell motility (104) (58) and endocytosis (104), as well as quorum sensing (12). PaxB is involved in a variety of actin-based processes including adhesion, motility, endocytosis, and cell sorting (20) (8). As RnoA, PldB, and PaxB all are involved in actin-mediated processes at approximately similar times during development, it is possible that these proteins function in the same pathway or potentially form a protein complex.

5.2 PaxB and PldB are involved in calcium dependent and independent cell-cell cohesion.

D. discoideum employs several cell adhesion systems to ensure proper development. These systems can be characterized as calcium dependent or independent, based upon their sensitivity or resistance to the calcium chelator EDTA, respectively. PaxB has previously been implicated in calcium dependent cell-cell cohesion (20). To determine if PldB is also involved in calcium mediated adhesion, or cell-cell adhesion in general, the cohesiveness of wild type cells, PaxB mutant cells, and PldB mutant cells was assessed. After four hours, starved cell aggregates were disrupted and then allowed to reform in the absence or presence of 10 mM EDTA over the course of 60 minutes (**Supplementary Figure 1**). Samples were taken after 60 minutes and the number of cohesive cells was determined. Consistent with previous findings (79), 40% of the wild type cells are found in cohered groups (**Figure 16A**). The presence of 10 mM EDTA greatly diminishes cohesion to approximately 15%. *paxB* null (PaxB$^-$) cells exhibit greater cell-cell cohesion than wild type cells, achieving 75% cohesion. The presence of EDTA does somewhat reduce the cohesion of the PaxB$^-$ cells, but over 55% cohesion is still retained. *pldB*

null (PldB$^-$) cells behave similarly to PaxB mutants, reaching over 70% cohesion and retaining over 55% cell-cell cohesion in the presence of EDTA. Cells overexpressing *pldB* (PldB OE) display over 60% cell-cell cohesion. However, unlike PldB$^-$ cells, PaxB$^-$ cells, or wild type cells, the cell-cell cohesion of PldB OE cells does not decrease in the presence of EDTA, suggesting this adhesion is EDTA insensitive.

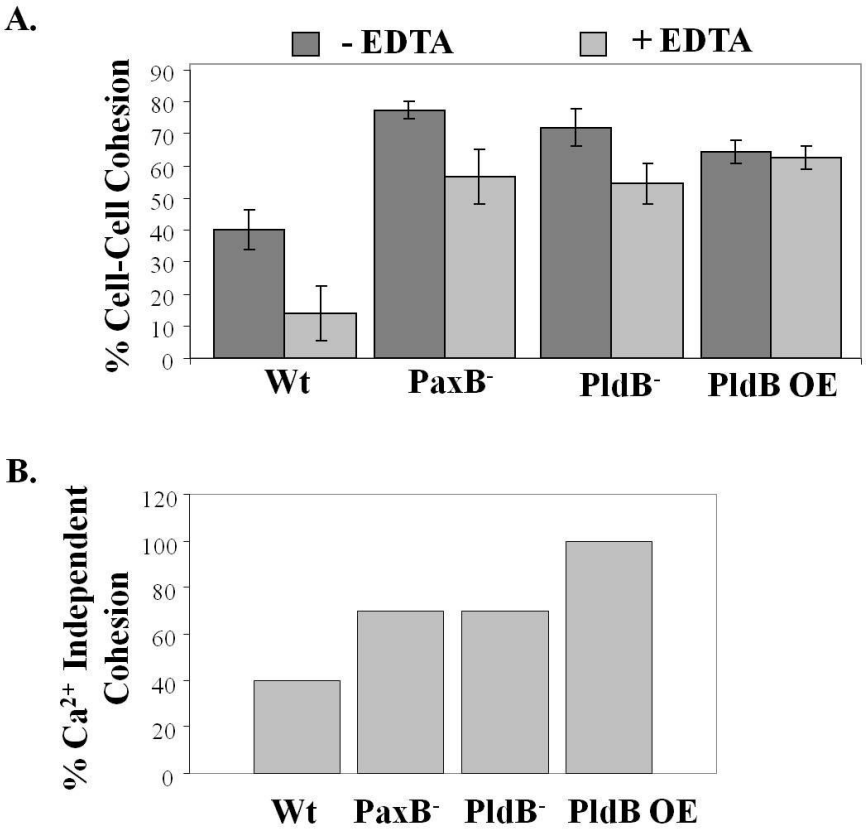

Figure 16: PaxB and PldB are involved in cell-cell cohesion. (A) After 4 hours of starvation in shaking culture, wild type (Wt) and mutant cell aggregates were disrupted and then allowed to reform in the absence or presence of 10 mM EDTA. After 60 minutes, the number of single and duplex cells was counted and the percentage of cell agglomeration was calculated. (B) Percentage of total cell-cell cohesion that is calcium independent.

In the absence of EDTA, the observed cell-cell cohesion is a measure of both calcium dependent and independent adhesion. As EDTA quenches calcium dependent adhesion, cell-cell cohesion measured in the presence of EDTA is representative of the amount of calcium

independent adhesion. To quantify the contribution of calcium independent adhesion to overall adhesion, the amount of calcium independent adhesion (adhesion with EDTA) was calculated as a percentage of total adhesion (adhesion without EDTA) for each cell line (**Figure 16B**). Calcium independent cohesion accounts for approximately 40% of the total cohesion in wild type cells, indicating the majority of cell-cell cohesion is calcium dependent. Approximately 70% of the total amount of cell-cell cohesion is calcium independent in both PaxB$^-$ and PldB$^-$ cells, suggesting that the elevated cohesion in these mutants is primarily due to increased calcium independent adhesion. PldB OE cells, which are EDTA insensitive, exclusively utilize calcium independent adhesion. Thus, all of the mutants tested display increased calcium independent cell-cell cohesion.

Alteration of the expression levels of PaxB and PldB interferes with the process of cell-cell cohesion. PaxB$^-$, PldB$^-$, and PldB OE cells all exhibit an increase in cohesion compared to wild type cells. While EDTA does reduce the elevated cell-cell cohesion, both PaxB$^-$ and PldB$^-$ cells retain over 50% cohesion. PldB OE cells appear resistant to EDTA, as cohesion was unaffected by its addition. PaxB$^-$, PldB$^-$, and PldB OE cells display a higher percentage of calcium independent adhesion compared to wild type cells. Taken together, the data suggest PaxB and PldB mediate cell-cell cohesion through calcium dependent and calcium independent pathways, respectively.

5.3 RnoA interacts with PaxB and PldB.

As mammalian ARNO, PLD, and paxillin localize to the actin cytoskeleton and participate in the same actin-driven processes, these proteins may potentially interact. To investigate this possibility, protein-protein interactions among their *Dictyostelium discoideum*

homologs, RnoA, PldB, and PaxB, respectively, were explored utilizing co-immunoprecipitation studies. Wild type cells and mutant cells were harvested, lysed, and incubated with antibodies against RnoA, PldB, or PaxB. A Western blot was then performed on the samples to identify co-immunoprecipitated proteins. As seen in **Figure 17A**, PaxB immunoprecipitated samples probed for the presence of RnoA by Western blot contain RnoA. In addition, PaxB immunoprecipitates also contain PldB, as indicated by Western blot. To confirm that PaxB was immunoprecipitated in these samples, PaxB immunoprecipitates from wild type cells and $PaxB^-$ cells were probed for PaxB by Western blot. PaxB was detected in the wild type immunoprecipitates, while PaxB was absent in the $PaxB^-$ samples. Taken together, this suggests that PaxB can be immunoprecipitated and that PaxB immunoprecipitates both RnoA and PldB. A Western blot performed on PldB immunoprecipitates detected the presence of RnoA in the sample (**Figure 17B**). Similarly, RnoA immunoprecipitates contain PldB as seen by a Western blot targeting PldB (**Figure 17C**). This demonstrates that RnoA immunoprecipitates PldB and that PldB is also able to immunoprecipitate RnoA. To confirm that RnoA was immunoprecipitated, RnoA immunoprecipitated samples were probed for RnoA by Western blot. Taken together, these studies suggest the existence of a protein complex between RnoA, PldB, and PaxB.

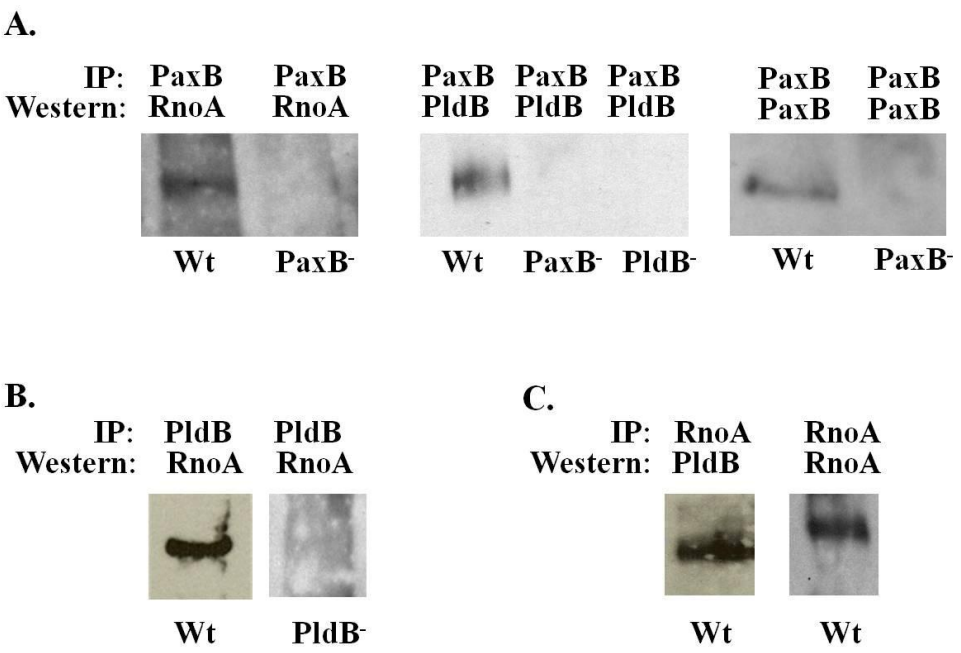

Figure 17: RnoA, PldB, and PaxB co-immunoprecipitate. 1 x 10^7 cells were lysed and incubated with antibodies overnight, followed by a 1hr incubation with beads. After washing, Western blots were performed on the immunoprecipitated products. (A) PaxB immunoprecipitation in wild type and mutant cells. (B) PldB immunoprecipitation in wild type and mutant cells. (C) RnoA immunoprecipitation in wild type cells.

5.4 RnoA-PldB-PaxB interaction is not mediated by PldB or PaxB.

The observed protein complex of RnoA, PldB, and PaxB could be the result of several distinct protein-protein interactions. The proteins could be linked through binding to the same protein and not through a protein complex. For example, protein A could bind protein C while protein B, independent of protein A, could also bind protein C (**Figure 18 I**). A second alternative could be that one protein serves as a connecting molecule between the other two proteins, such that the complex does not exist in the absence of this protein. For example, both protein A and protein C bind to protein B, but protein A and protein C do not physically interact (**Figure 18 II**). In this case, in the absence of protein B, protein A and protein B would not interact. The third potential type of interaction would be that all three proteins physically

associate and that this interaction is not dependent upon a single protein. For instance, protein A binds both protein B and protein C, protein B binds both protein A and protein C, and protein C binds both protein A and protein B (**Figure 18 III**). In such a situation, the absence of one protein would not prohibit the other two complex members from binding.

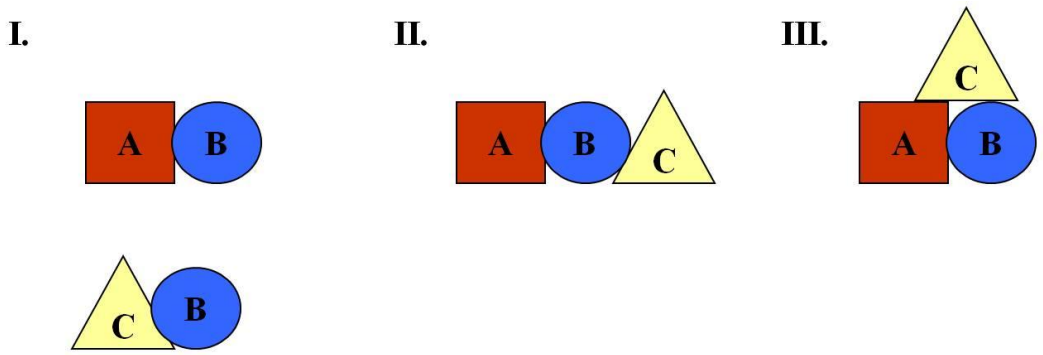

Figure 18: Scheme of potential RnoA, PldB, PaxB interactions. (I) A and C do not interact, instead both bind B. (II) The interaction of A and C is mediated by B. (III) A, B, and C all bind.

To determine if one protein serves as a connection between the other two proteins, as depicted in **Figure 18 II**, the dependency of the RnoA-PldB-PaxB complex on a single protein was assessed. To determine if PldB is required for RnoA and PaxB protein-protein interactions, PaxB was immunoprecipitated in wild type and PldB$^-$ cells under both vegetative and developmental conditions. Western blots probing for RnoA were then performed on the samples. As seen in **Figure 19A**, RnoA was immunoprecipitated by PaxB in both wild type and PldB$^-$ cells under both vegetative and starved conditions. Thus, RnoA and PaxB are able to interact in the absence of PldB suggesting that PldB is not needed for RnoA and PaxB interaction. To ascertain if PaxB mediates the interaction between RnoA and PldB, RnoA was immunoprecipitated in wild type and PaxB$^-$ cells and a Western blot probing for PldB was

performed. As shown in **Figure 19B**, RnoA immunoprecipitates from both wild type and PaxB$^-$ cells contain PldB, implying that the PaxB is not required for RnoA to immunoprecipitate PldB. Taken together, the results suggest that the interactions among RnoA, PldB, and PaxB are not mediated by either PldB or PaxB.

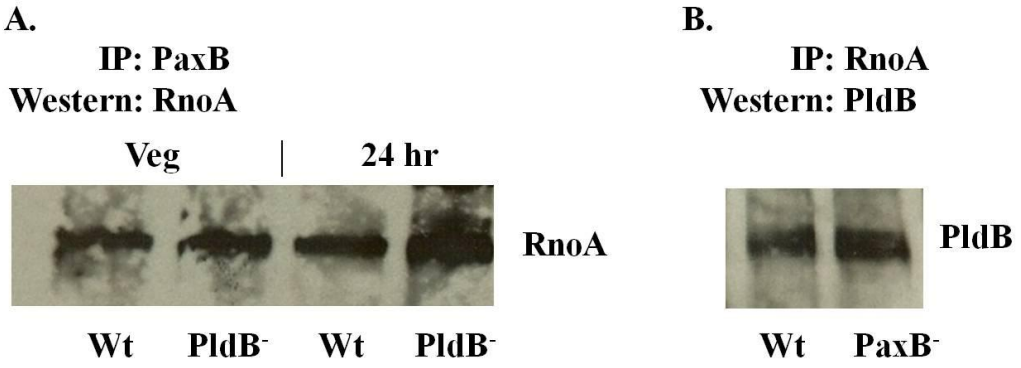

Figure 19: RnoA, PldB, and PaxB interactions are not dependent on PldB or PaxB. (A) PaxB was immunoprecipitated in vegetative and starved wild type and PldB$^-$ cells. A Western blot probing for RnoA was then performed in the immunoprecipitated samples. (B) RnoA was also immunoprecipitated in wild type and PaxB$^-$ cells. A Western blot probing for PldB was performed on the immunoprecipitated samples.

5.5 RnoA-PaxB-PldB interaction is not dependent on F-actin organization.

Given that RnoA, PldB, and PaxB all co-localize with the actin cytoskeleton, the observed protein interactions could be a consequence of these proteins binding the actin cytoskeleton, not an RnoA-PldB-PaxB association. To distinguish between these two possibilites, cells were immunoprecipitated following the disruption of filamentous actin organization by Latrunculin A treatment. To confirm that the actin cytoskeleton was disrupted, aliquots of treated cells were stained for F-actin (red) with Rhodamine Phalloidin and nuclei (blue) with To-Pro. As determined by confocal microscopy, F-actin organization was reduced with 3 µM Latrunculin A and completely disrupted with 10 µM Latrunculin A as evidenced by the loss of Phalloidin staining in **Figure 20A**.

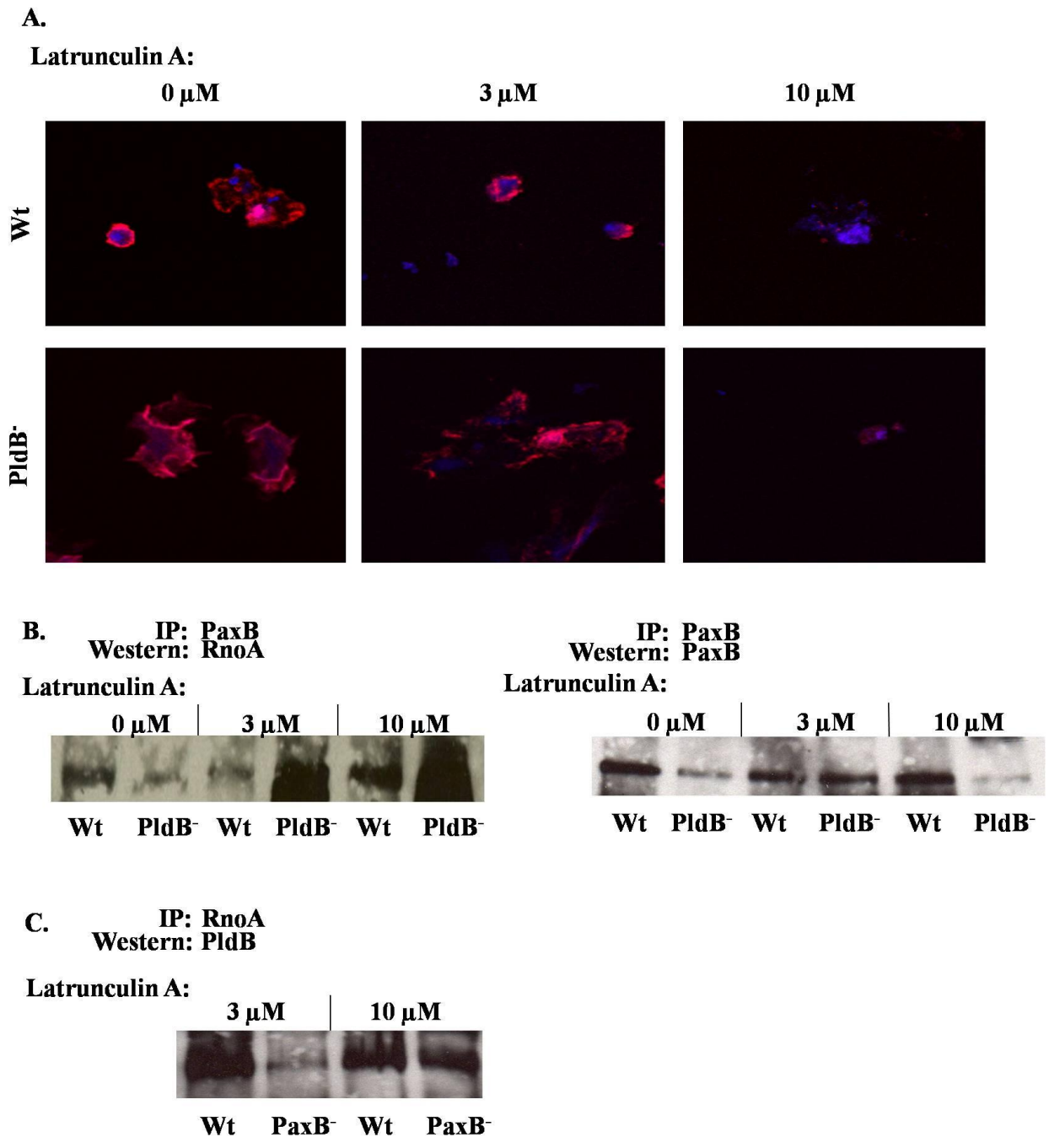

Figure 20: F-actin organization is not required for RnoA, PldB, and PaxB to interact. (A) Wild type and PldB$^-$ cells treated with LatrunculinA were incubated with Rhodamine Phalloidin (red) and To-Pro (blue) to stain for F-actin and nuclei, respectively. (B) Latrunculin A treated wild type and PldB$^-$ cells were immunoprecipitated with PaxB. A Western blot was performed on the immunoprecipitated samples probing for RnoA. The blot was also probed for the presence of PaxB. (C) Latrunculin A treated wild type and PaxB$^-$ cells were immunoprecipitated with RnoA. A Western blot probing for PldB was performed on the immunoprecipitated samples.

Having confirmed the disruption of F-actin, samples were then immunoprecipitated with antibodies targeting PaxB in both wild type and PldB$^-$ cells. A Western blot probing for RnoA was then performed (**Figure 20B**). To demonstrate that PaxB was in fact immunoprecipitated, the samples were also probed for the presence of PaxB. PaxB was detected in all samples, indicating PaxB was immunoprecipitated. In both wild type and PldB$^-$ cells not treated with Latrunculin A, RnoA was found in the PaxB immunoprecipitated product. PaxB was also found to immunoprecipitate RnoA in wild type and PldB$^-$ cells treated with either 3 µM or 10 µM Latrunculin A. As treatment with Latrunculin A disrupted the actin cytoskeleton, but did not disrupt RnoA and PaxB co-immunoprecipitation, these proteins are interacting independent of the actin cytoskeleton. Given that RnoA and PaxB still co-immunoprecipitate in PldB$^-$ cells, the loss of PldB does not appear to rupture RnoA-PaxB interactions, again indicating PldB is not necessary for an interaction to occur.

Along with wild type cells, cells lacking PaxB were also treated with 3 µM or 10 µM Latrunculin A then immunoprecipitated for RnoA. A Western blot probing for PldB was performed on the samples (**Figure 20C**). PldB was present in RnoA immunoprecipitates treated with either concentration of Latrunculin A in both wild type and PaxB$^-$ cells. Thus, RnoA and PldB are able to interact in the absence of F-actin organization or PaxB. Taken together, the data suggest the protein interactions among RnoA, PldB, and PaxB are independent of actin cytoskeletal organization and provide further evidence that these interactions are not mediated by either PldB or PaxB.

5.6 PaxB and PldB interact to regulate cell-substrate adhesion.

As RnoA, PldB, and PaxB appear to physically interact, these proteins may also share a genetic interaction. To determine whether a genetic link between RnoA, PldB and PaxB exists, the role of these proteins in the actin-driven process of cell-substrate adhesion was examined. Wild type and mutant cells were allowed to adhere to a glass surface and then gently agitated. The non-adhered cells in the supernatant were counted and subtracted from the total cell number as a measure of cell-substrate adhesion. As depicted in **Figure 21A**, approximately 80% of wild type cells adhere to the substratum. Both PldB OE cells and PldB$^-$ cells exhibit cell-substrate adhesion comparable to wild type cells. Consistent with the literature (8), PaxB$^-$ cells are significantly less adhesive to the substratum than wild type cells with only 50% of the cells adhering to the substrate. Interestingly, the overexpression of *pldB* in cells lacking *paxB* returns adhesion to the wild type level of 80% adhesion suggesting that PldB overproduction compensates for the loss of PaxB during cell-substrate adhesion. Given that the overexpression of *pldB* in *paxB* null cells generates the adhesion phenotype of the PldB OE cells, *paxB* and *pldB* likely engage in an epistatic relationship.

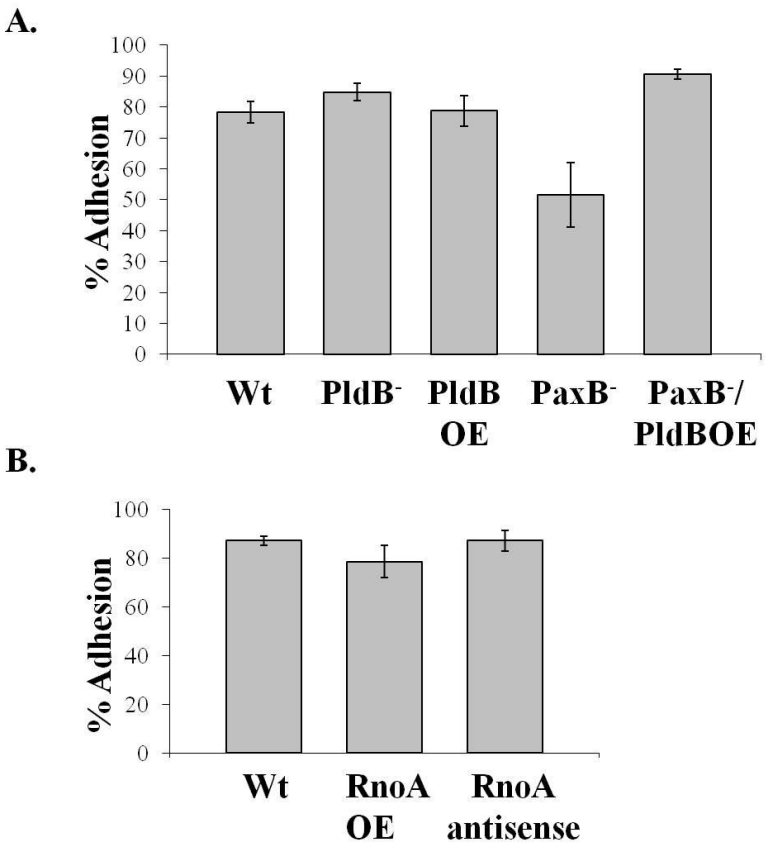

Figure 21: Overexpression of PldB rescues cell-substratre adhesion of PaxB- cells. 1 x 10^6 cells were allowed to adhere to a glass surface for 2 hrs. After gentle agitation, the number of cells in the supernatent was counted and the percent of adhered cells calculated. (A) The adhesion defect observed in *paxB* null cells is rescued by overexpressing PldB. (B) RnoA mutant cells have cell-substrate adhesion comparable to wild type cells.

As described in earlier chapters, RnoA mutant cells have developmental defects. RnoA OE cells arrest at the mound stage, while RnoA antisense cells have a prolonged aggregation stage. Given that cell adhesion is involved in various stages of development, particularly during aggregation and mound formation, defects in adhesion can result in abnormal development. To determine if adhesion deficiencies may contribute to the observed developmental phenotypes, the cell-substrate adhesion of the RnoA mutant cells was examined. As seen in **Figure 21B**, RnoA OE and RnoA antisense cells both have cell-substrate adhesion comparable to that of wild type cells. This suggests that alteration of RnoA production does not interfere with cell-substrate

adhesion. As RnoA antisense cells and RnoA OE cells do not exhibit impaired cell-substrate adhesion, adhesion defects are not likely a contributing source to the abnormal developmental phenotypes characteristic of these cells.

5.7 Discussion.

Given that ARNO, PLD, and paxillin have been associated with actin-based processes in mammalian cells, the potential exists for these proteins to function in the same pathway or even to physically interact. To investigate these possibilities, the relationship between the *D. discoideum* ARNO, PLD, and paxillin homologs in actin-processes was determined. As PaxB has been linked to cell-cell cohesion, the role of PldB in this process was assessed. Like the PaxB OE cells described by Duran et al (20), PaxB$^-$ cells, PldB$^-$ cells, and PldB OE cells all exhibit an increase in cell-cell cohesion compared to wild type cells. While the presence of EDTA reduces wild type cohesion to less than 15%, these mutants all maintain levels of cohesion exceeding 55%, indicating the observed increase in cell-cell cohesion is primarily due to calcium independent adhesion mechanisms. While the total amount of wild type cell adhesion was calculated to consist of 40% calcium independent adhesion, adhesion in both PaxB$^-$ and PldB$^-$ cells is comprised of 70% calcium independent adhesion. The PldB OE mutants are distinct from the other cell lines tested in that addition of EDTA does not decrease the elevated cohesion, suggesting that the overexpression of PldB suppresses calcium dependent adhesion and invokes only calcium independent adhesion. This implies a role for PldB in calcium independent adhesion. As the overexpression of PaxB was previously reported to elevate cell cohesion through a calcium dependent pathway (20), PaxB is likely involved in calcium dependent adhesion. Taken together, the data show that PaxB and PldB are both involved in cell-cell

cohesion and appear to utilize calcium dependent and independent pathways, respectively, to mediate this process.

In *D. discoideum*, several distinct adhesion systems operate throughout the course of development to facilitate the transition from a population of single cells to a multicellular structure. The initial adhesion molecule expressed, DdCAD-1 or gp24, is encoded by the *cadA* gene and mediates a calcium dependent adhesion system from the onset of starvation through culmination (7) (84). A calcium independent adhesion system is moderated by gp80. Gp80 expression increases between 4 and 12 hours into development, which corresponds to the stages between cell streaming and mound formation (61) (84). As a cell enters into the developmental program, DdCAD-1 is present at the cell periphery, particularly in membrane protrusions containing F-actin (80). During cell aggregation, DdCAD-1 disappears from these regions while gp80 simultaneously accumulates (80). The dynamics of DdCAD-1 localization highlight the transient nature of cell-cell adhesion. DdCAD-1 is believed to play a role in recruitment of cells into streams, while gp80 strengthens cell-cell contacts (84).

The adhesion systems mediated by DdCad-1 and gp80 are both active during the time period over which cell-cell cohesion was examined. Thus, PldB and PaxB may potentially participate in these adhesion systems as cell-cell cohesion studies implicate PldB in calcium independent adhesion and PaxB in calcium dependent adhesion. In addition, both PldB and PaxB mutants display many of the same pheonotypic defects observed in DdCAD-1 and gp80 mutants. For instance, PaxB OE cells, PaxB$^-$ cells, and *cadA* null cells have cell sorting defects and reduced spore viability (8) (20) (84) (100). Also, the loss of gp80 or of PLD activity, reduces cell motility (104) (84). PaxB and PldB may therefore participate in DdCAD-1 and gp80 signaling pathways to regulate cell-cell adhesion.

Cell-surface adhesion molecules such as DdCAD-1 and gp80 signal to downstream targets which in turn coordinate actin cytoskeletal rearrangements to enable cell-cell adhesion. Given the observed cell-cell cohesion in mutant cell lines and that PldB and PaxB co-localize with F-actin, PldB and PaxB potentially contribute to the cytoskeletal remodeling required for cell-cell contacts to occur. Specifically, PldB and PaxB are likely involved in sensing and regulating cell-cell adhesion. As the dynamic nature of cell-cell contacts mandates constant changes in a cell's cohesiveness, tight control and coordination of the multiple adhesion systems involved is essential. Since alteration of PldB or PaxB production results in increased adhesion, these proteins may regulate calcium independent and calcium dependent cell cohesion pathways through crosstalk between these adhesion systems. As depicted in **Figure 22**, PaxB positively regulates calcium dependent adhesion. The increase in calcium dependent adhesion may negatively regulate calcium independent adhesion either directly or indirectly. The overproduction of PaxB would increase calcium dependent adhesion and reduce calcium independent adhesion. The loss of PaxB would reduce calcium dependent adhesion, but increase calcium independent adhesion. Either the overproduction or the loss of PaxB would result in increased cell cohesion. PldB appears to negatively regulate calcium dependent adhesion, while promoting calcium independent adhesion. The loss of PldB removes inhibition of calcium dependent adhesion, resulting in increased activity in this adhesion system. The overproduction of PldB effectively blocks all calcium dependent adhesion, generating only calcium independent adhesion. Since both DdCAD-1 and gp80 adhesion systems are active during the time point tested, PldB and PaxB may be involved in regulating both systems through crosstalk in adhesion machinery to ensure proper cell-cell cohesion.

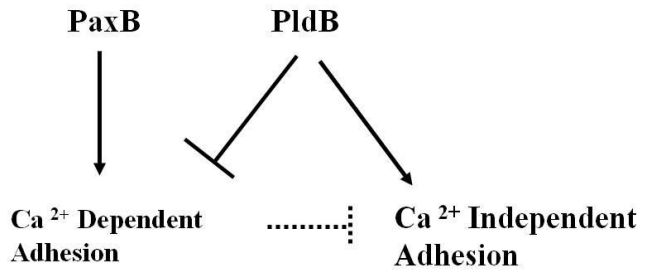

Figure 22: PaxB and PldB both regulate cell adhesion. PaxB positively regulates calcium dependent adhesion, which may down regulate calcium independent adhesion. PldB negatively regulates calcium dependent adhesion, which serving as a positive regulator for calcium independent adhesion.

Given their common localization and participation in actin-based processes, the possibility of a physical association between PldB and PaxB exists. Co-immunoprecipitation studies were utilized to explore the physical relationship between PldB and PaxB, as well as RnoA. PaxB was found to immunoprecipitate both PldB and RnoA. Additionally, PldB was able to immunoprecipitate RnoA and RnoA immunoprecipitates PldB. As RnoA, PldB, and PaxB all co-immunoprecipitate, these proteins likely form a protein complex.

To further characterize the interaction between RnoA, PldB, and PaxB, the dependency of this association on a single protein was assessed. PaxB and RnoA are able to co-immunoprecipitate in the absence of PldB, suggesting that PldB is not responsible for the interaction between PaxB and RnoA. RnoA and PldB co-immunoprecipitate in the absence of PaxB, implying that PaxB does not mediate RnoA and PldB binding. Thus, the interaction between RnoA, PldB, and PaxB is not mediated by PldB or PaxB. To confirm that RnoA, PldB, and PaxB are not associated through the actin cytoskeleton, Latrunculin A treatment was applied to disrupt F-actin organization prior to immunoprecipitation. After Latrunculin A treatment, PaxB is still able to immunoprecipitate RnoA in absence of F-actin organization. Also, RnoA can immunoprecipitate PldB after F-actin disruption. Therefore, the loss of actin cytoskeletal organization did not prevent RnoA, PldB, and PaxB from associating. Taken together, these

studies indicate that the interaction between RnoA, PldB, and PaxB is not mediated by PldB, PaxB, or an association with the actin cytoskeleton. These results lend further credence to the possibility of RnoA, PldB, and PaxB forming a complex.

The possibility of RnoA mediating the interaction between PldB and PaxB still remains. However, lack of an *rnoA* null mutant makes testing this possibility impossible. Wild type cells and RnoA antisense cells, which produce less RnoA, could be immunoprecipitated with PaxB antibodies and then a Western blot probing for PldB could be performed. The amount of PldB detected in the RnoA antisense cells could be compared to that of the wild type cells. A reduction in detected PldB may indicate RnoA mediates the interaction between PldB and PaxB. The detection of similar levels of PldB in immunoprecipitates from both cell lines would suggest the interaction between PldB and PaxB is not dependent upon RnoA.

As evidence suggests RnoA, PldB, and PaxB physically interact, the possibility of a genetic interaction during cell-substrate adhesion was explored. RnoA mutants and PldB mutants both display cell-substrate adhesion comparable to that of wild type cells, at approximately 80% adhesion. This indicates that alteration of RnoA or PldB protein levels does not disrupt cell-substrate adhesion. The overexpression of PldB, however, rescues the known adhesion defect of PaxB$^-$ cells, implying a genetic interaction between *pldB* and *paxB*. In mammalian systems, paxillin is known to recruit the necessary components to sites of cell-substrate adhesion (17, 77). PaxB may therefore serve to recruit PldB to the site of cell-substrate adhesion as depicted in **Figure 23**. In the absence of PaxB, PldB might not be in the vicinity to participate in adhesion. The abundance of PldB in PaxB$^-$/PldB OE cells may override the need for PaxB to properly localize PldB, as the excess PldB may be accessible to cell-substrate adhesion sites.

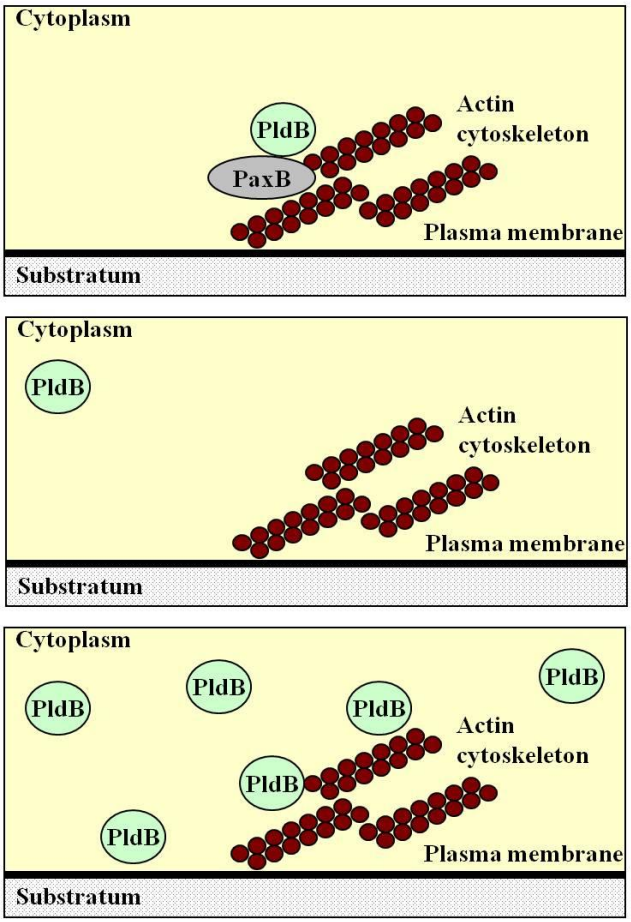

Figure 23: PaxB and PldB mediate cell-substrate adhesion. In wild type cells, PaxB serves as a scaffold to recruit PldB to sites of actin organization and cell-substrate adhesion. In the absence of PaxB, PldB may not properly localize to areas of adhesion . The overexpression of PldB in cells lacking PaxB (PaxB$^-$/PldB OE) generates excessive levels of PldB which likely localize to adhesion areas without PaxB.

Taken together, these results argue a role for RnoA, PldB, and PaxB in the coordination of cytoskeletal rearrangements in actin-based processes such as adhesion. The findings observed in *D. discoideum* can bring new insights to mammalian systems as the homologs of RnoA, PldB, and PaxB have been associated to a wide variety of actin dependent processes. While the individual roles of these proteins has been studied, and evidence hints at the existence of a complex, the direct interaction of ARNO, PLD, and paxillin has not been explored in mammalian cells. A functional understanding of such a complex can shed light on cellular processes such as adhesion and motility, which are commonly altered in malignant cells.

CHAPTER 6: Summary

Regulation of actin cytoskeletal organization is the foundation for many cellular processes. We present evidence that *Dictyostelium discoideum* RnoA plays a key role in the regulation of the actin cytoskeleton and in actin dependent processes throughout development. RnoA is present throughout all stages of the *D. discoideum* life cycle, but is highly expressed during cell aggregation and mound formation suggesting that RnoA may play a role during these developmental stages. Consistent with this, we find that the overproduction or reduction of RnoA results in abnormal developmental phenotypes. High levels of RnoA are likely needed for cell aggregation as cells with reduced RnoA levels have an extended aggregation stage, leading to delayed development. These levels of RnoA must decrease for development beyond the mound stage to occur as cells with artificially elevated levels of RnoA arrest at the mound stage of development

The mound arrest of the RnoA OE cells can be rescued by the addition of wild type cells. This implies that while RnoA OE cells are unable to produce the necessary developmental signals, they can respond to these signals when produced by wild type cells. The preferential localization of RnoA OE cells to the stalk in these chimeric mixtures suggests that RnoA OE cells may have deficiencies in prespore cell differentiation. Thus, RnoA may play a role in prespore cell differentiation or sorting during development.

The observed developmental defects of the RnoA mutant cells may be rooted in cAMP chemotactic deficiences. Both RnoA antisense cells and RnoA OE cells fail to undergo cell streaming, a process driven by effective cAMP chemotaxis. In addition, these mutants do not chemotax toward cAMP. As cell motility and folate chemotaxis are not impaired in these mutants, alteration in RnoA production specifically affects cAMP chemotaxis. RnoA antisense

cells and RnoA OE cells likely adhere to neighboring cells during development rather than undergoing cAMP-directed chemotaxis and cell streaming. RnoA appears to influence a cell's ability to sense cAMP as RnoA mutant cells do not exhibit the characteristic drop in speed after global stimulation with cAMP. These mutants also do not polarize like wild type cells in the presence of a cAMP gradient. In addition, RnoA antisense cells and RnoA OE cells polymerize F-actin differently than wild type cells in response to cAMP stimulation. Like its mammalian homolog ARNO, RnoA likely exerts its influence on a cell through upstream regulation of the actin cytoskeleton. RnoA OE cells were observed to have altered F-actin organization and increased filopodia. These differences in F-actin localization may interfere with a cell's ability to polarize and undergo effective chemotaxis and cell streaming as the intracellular machinery is not properly positioned to relay the appropriate signals for these processes to occur.

Like mammalian ARNO, RnoA also appears to regulate organization of the actin cytoskeleton. Given these similarities, a new avenue for exploring many of the unknown signaling and regulatory events surrounding ARNO can be examined using *D. discoideum* RnoA as a model. For instance, ARNO has been shown to activate PLD activity in epithelial cells (70), yet the precise mechanism of action remains to be elucidated. This question can readily be addressed by decoding the signaling pathway of RnoA and the PLD homolog, PldB. Given the relative ease of genetically modifying *D. discoideum*, the RnoA domains involved in this signaling can be mapped by developing various mutations in the *rnoA* gene.

RnoA, PldB, and PaxB, the paxillin homolog all co-localize to the actin cytoskeleton and participate in actin dependent processes. As demonstrated by co-immunoprecipitation studies, RnoA, PldB, and PaxB all co-immunoprecipitate. These results suggest that in addition to PaxB and PldB being interaction partners of RnoA, these proteins also form a complex. The protein

complex of RnoA, PldB, and PaxB is not mediated by PldB, PaxB, or an association with the actin cytoskeleton.

PldB and PaxB both regulate cell-cell cohesion through calcium independent and calcium dependent pathways, respectively, and may therefore participate in DdCad-1 and gp80 mediated adhesion systems. As the alteration of either PldB or PaxB expression levels induces an increase in cell-cell adhesion, a complex crosstalk between calcium dependent and calcium independent adhesion systems appears to exist. PldB and PaxB may serve as sensors to maintain tight regulation and balance between different adhesion mechanisms. Furthermore, a genetic interaction exists between *pldB* and *paxB* as the overexpression of *pldB* rescues the cell substrate adhesion defect of PaxB$^-$ cells. This finding supports a model where PaxB recruits PldB to sites of adhesion. The absence of PaxB likely prevents proper PldB localization for cell-substrate adhesion. The overproduction of PldB in PaxB$^-$/PldB OE cells compensates for the loss of PaxB as now the excessive PldB present in the cell may localize to the site of cell-substrate adhesion without the recruitment of PaxB.

The work presented here implicates RnoA, a putative GEF, as a vital regulator for cellular response to cAMP during early development. It can be supposed that upon cAMP stimulation, RnoA activates its target to allow proper actin cytoskeletal organization, enabling chemotaxis to occur. A reduction in RnoA levels dampens this signaling, but residual RnoA signals to downstream targets, leading to proper actin organization and allowing development to occur but with a significant delay. As endogenous RnoA levels decrease after the mound stage, the overproduction of RnoA floods the pathway with excess signaling, preventing normal development past the mound, while causing rearrangement of the actin cytoskeleton to form filopodia. These results also identify PldB and PaxB as interaction partners of RnoA. RnoA,

PldB, and PaxB form a protein complex which likely functions to coordinate cytoskeletal organization in actin-based processes such as adhesion.

Given its extensive role in a cell, a clear and thorough understanding of actin cytoskeletal regulation and organization is fundamental to demystifying the complex network of signal transduction pathways that coordinate physiological processes. This work highlights the role of RnoA as an integral player in relaying chemotactic signals to coordinate the actin cytoskeleton. An understanding of RnoA can shed light on the signaling events that culminate in *Dictyostelium discoideum* development as well as those involved in mammalian systems.

CHAPTER 7: Future directions

The work presented here generates new avenues for understanding the signal transduction pathways governing the regulation and organization of the actin cytoskeleton in mammalian systems by utilizing the *Dictyostelium discoideum* homolog of ARNO, RnoA, a guanine nucleotide exchange factor functionally associated with the actin cytoskeleton. Future work can build upon the discussed data to further delineate the mechanistic function and role of RnoA, as well as its relationship to PldB and PaxB, the homologs of mammalian phospholipase D and paxillin, respectively.

Mammalian ARNO harbors nucleotide exchange capabilities owing to its central catalytic Sec7 domain. As RnoA contains a highly conserved Sec7 domain, RnoA may also be capable of nucleotide exchange activity. A nucleotide exchange activity assay could be utilized to determine if RnoA, like its mammalian homolog, can catalyze the exchange of nucleotides. In such an assay the exchange rate of GDP for a non-hydrolysable GTP analog is measured in the presence of varying concentrations of purified or recombinant RnoA. In addition, if RnoA is catalytically active, the involvement of nucleotide exchange by RnoA in various developmental processes can be determined. For instance, point mutations can be introduced into the Sec7 domain of the *secg* gene in order to produce a catalytically inactive RnoA mutant. For physiologically processes where a catalytically active Sec7 domain of ARNO is required, the RnoA mutant will have altered performance compared to wild type cells as well as RnoA OE cells. Determining which processes involve RnoA's catalytic function can help establish the mechanistic role of RnoA in these processes.

The PH domain of mammalian ARNO is known to positively regulate the catalytic Sec7 domain through interactions with inositol phospholipids present in membranes (9). To determine

if the PH domain of RnoA also stimulates nucleotide exchange, the exchange activity of cells carrying a mutated *rnoA* gene lacking the PH domain can be compared to that of wild type cells. A change in the exchange activity of the mutant cells compared to wild type cells would indicate that the PH domain does regulate the Sec7 domain and in turn influences the nucleotide exchange properties of the protein.

Future work can also address the involvement and function of the PH domain and the ankyrin repeat domain of RnoA in protein-protein interactions. As both PH domains and ankyrin repeat domains are known to mediate protein-protein interactions, RnoA may interact with protein partners such as PldB and PaxB through either or both of these domains. To address this, truncated versions of RnoA can be generated with either the PH domain, the ankyrin repeat domain, or both domains missing from the final protein product. Co-immunoprecipiation studies can then be performed on cell lines carrying the truncated RnoA mutants to determine whether RnoA can still interact with PldB and PaxB. If loss of either the PH domain or the ankyrin repeat domain reduces or abolishes co-immunoprecipiation of RnoA and either PldB or PaxB, then that particular domain likely mediates RnoA's protein interactions.

As evidence presented here describes a role for PaxB and PldB in the regulation of calcium dependent and independent adhesion, these proteins may function in the DdCad and gp80 adhesion systems. DdCad positively regulates calcium dependent adhesion as the loss of *cadA*, the gene encoding DdCad, diminishes calcium dependent cell-cell cohesion (100). Our findings, along with the evidence that PaxB OE cells have elevated cell-cell cohesion due to an increase in calcium dependent adhesion (20), suggest that PaxB also positively mediates calcium dependent adhesion. To connect PaxB to calcium dependent adhesion mediated by DdCad, cell lines overexpressing *paxB* in a *cadA* null background (DdCad$^-$/PaxB OE) can be generated. The

percentage of cell-cell cohesion, in both the absence and presence of EDTA, of the DdCad$^-$/PaxB OE cells can then be determined. If the double mutant cell line displays reduced cell cohesion, like the DdCad$^-$ cells, then PaxB functions upstream of DdCad. If the double mutants have increased cell cohesion, then PaxB lies downstream of DdCad.

Similar studies could be performed to link PldB and the gp80 adhesion system. gp80 is believed to directly mediate calcium independent cell-cell adhesion as expression of gp80 results in an increase in cell cohesiveness (40) and the sequestration of gp80 through antibodies blocks calcium independent cohesion (82). As PldB promotes calcium independent cohesion during the same period of development in which gp80 is active, PldB may participate in the gp80 adhesion pathway. *pldB* could be overexpressed in cells lacking *csaA*, the gene encoding gp80. If the gp80$^-$/PldB OE mutant has decreased cell-cell cohesion, this would suggest that PldB lies downstream of gp80. Alternatively, if the gp80$^-$/PldB OE mutant has increased cohesion, then PldB likely functions upstream of gp80. Determining the adhesion system in which both PldB and PaxB participate can help establish the signaling events between adhesion mechanisms which regulate cellular adhesion.

As RnoA associates with PldB and PaxB, RnoA may also regulate adhesion through either calcium dependent or calcium independent mechanisms. Utilizing the RnoA mutant cell lines, the influence of increased or decreased RnoA levels on cell-cell cohesion can be determined. If the loss of RnoA correlates with reduced cell cohesiveness and the over production of RnoA increases cell cohesiveness, RnoA likely serves to positively regulate cell-cell cohesion. Alternatively, if the loss of RnoA increases cell cohesion and the over production of RnoA decreases cell cohesion, RnoA negatively regulates cell-cell cohesion. The involvement of RnoA in calcium dependent and calcium independent adhesion can be assessed by comparing the

percentage of cell-cell cohesion in the absence and presence of EDTA. Cell-cell cohesion in the absence of EDTA is a measure of the total cohesion from both calcium dependent and calcium independent systems. Cell-cell cohesion in the presence of EDTA is a measure of calcium independent adhesion. If RnoA mediates adhesion through a calcium dependent pathway, RnoA's impact on adhesion will be negated by the addition of EDTA. If RnoA contributes to adhesion through calcium independent channels, RnoA's effect on adhesion will be insensitive to EDTA. Given the complexity of PaxB and PldB's involvement with cell adhesion, RnoA may potentially influence both calcium dependent and independent adhesion.

As RnoA, PldB, and PaxB all co-localize with the actin cytoskeleton, the visualization of how these proteins localize in relation to each other could bring further insight to the role of this potential protein complex, particularly during cell adhesion. Utilizing immunofluoresence and plasmids encoding fluorescently-tagged proteins, RnoA, PldB, and PaxB can all be visualized in a single cell. For instance, GFP-labeled *rnoA* and YFP-labeled *pldB* can be transformed into wild type cells. These cells can then be incubated with PaxB antibodies and TRITC-labeled secondary antibodies, thus allowing RnoA, PldB, and PaxB to be visualized simultaneously in cells adhered to a glass slide. The co-localization of RnoA, PldB, and PaxB would further support the existence of a protein complex as well and may implicate a role for such a complex during cell-substrate adhesion.

The localization of PldB in cells lacking PaxB would also provide clues regarding how PldB compensates for the loss of PaxB. As suggested by the proposed model, the loss of PaxB likely impairs the proper localization of PldB during adhesion. The overproduction of PldB in these cells overrides the need for PaxB to direct PldB to sites of substrate adhesion. The

localization of cells over producing YFP-labeled PldB to sites of cell substrate adhesion would lend further support to the current model.

Given the genetic interaction between PldB and PaxB and the physical association of RnoA, PldB and PaxB, RnoA may also genetically interact with PaxB. To explore this possibility *rnoA* can be over expressed in cells lacking *paxB*. The percentage of PaxB$^-$/RnoA OE mutant cells adhered to the substratum can then be assessed. RnoA OE cells have cell-substrate adhesion comparable to that of wild type cells, while PaxB$^-$ cells are defective in cell-substrate adhesion. If the over production of RnoA rescues the adhesion defect due to the loss of PaxB in the PaxB$^-$/RnoA OE cells, then RnoA and PaxB genetically interact. PaxB may also then be involved in the localization of RnoA during adhesion. By comparing the localization of GFP-labeled RnoA in wild type cells and PaxB$^-$ cells, the influence of PaxB on RnoA localization during cell-substrate adhesion can be determined.

The findings presented here highlight the relationship between RnoA, PldB, and PaxB in *Dictyostelium discoideum*. Therefore, the relationship of their mammalian homologs during processes such as cellular adhesion and migration merits exploration. It would be of particular interest to examine the relationship between PLD and paxillin, the PldB and PaxB homologs, respectively, in cell lines with altered adhesion and migration properties such as often occurs in cancer cells. As PLD and paxillin genetically interact in *D. discoideum*, a similar interaction may be observed in cancerous mammalian cells. The interplay between ARNO, PLD, and paxillin during adhesion and migration can help elucidate the mechanistic properties of a malignant cell and may potentially open new target areas for cancer drug development.

SUPPLEMENTARY FIGURES

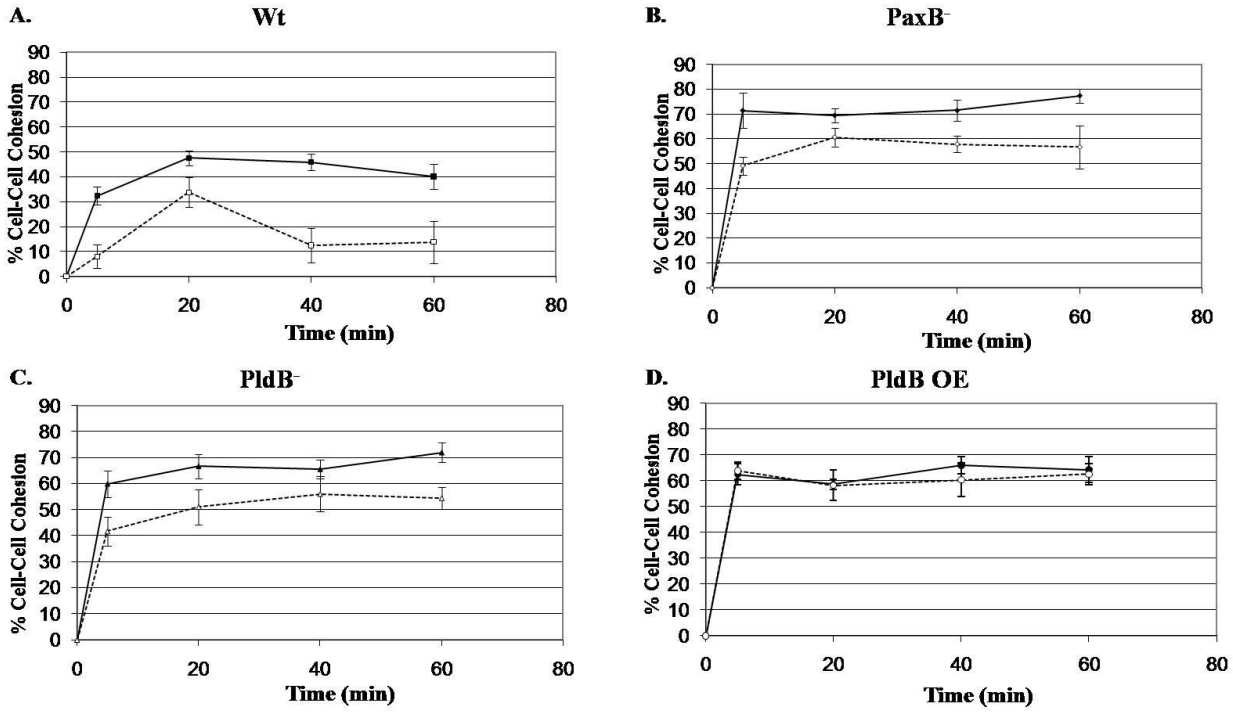

Supplementary Figure 1: Time course of cell-cell cohesion. After 4 hours of starvation in shaking culture, wild type (Wt) and mutant cell aggregates were disrupted and then allowed to reform in the absence (solid lines) or presence (dashed lines) of 10 mM EDTA. At various time points, the number of single and duplex cells was counted and the percentage of cell agglomeration was calculated.

REFERENCES

1. Araki, T., T. Abe, J. G. Williams, and Y. Maeda. 1997. Symmetry breaking in Dictyostelium morphogenesis: Evidence that a combination of cell cycle stage and positional information dictates cell fate. Dev. Biol. 192:645-648.

2. Arigoni, M., E. Bracco, D. F. Lusche, H. Kae, G. Weeks, and S. Bozzaro. 2005. A novel Dictyostelium RasGEF required for chemotaxis and development. BMC Cell Biol. 6:43:18 pages.

3. Assinder, S. J., J. A. Stanton, and P. D. Prasad. 2009. Transgelin: an actin-binding protein and tumour suppressor. Int J Biochem Cell Biol 41:482-486.

4. Bagorda, A., V. A. Mihaylov, and C. A. Parent. 2006. Chemotaxis: moving forward and holding on to the past. Thromb. Haemost. 95:12-21.

5. Blaauw, M., M. H. Linskens, and P. J. van Haastert. 2000. Efficient control of gene expression by a tetracycline-dependent transactivator in single Dictyostelium discoideum cells. Gene 252:71-82.

6. Bouschet, T., S. Martin, V. Kanamarlapudi, S. Mundell, and J. M. Henley. 2007. The calcium-sensing receptor changes cell shape via a beta-arrestin-1 ARNO ARF6 ELMO protein network. J Cell Sci 120:2489-2497.

7. Brar, S. K., and C. H. Siu. 1993. Characterization of the cell adhesion molecule gp24 in Dictyostelium discoideum - mediation of cell-cell adhesion via a Ca2+-dependent mechanism. J. Biol. Chem. 268:24902-24909.

8. Bukharova, T., G. Weijer, L. Bosgraaf, D. Dormann, P. J. van Haastert, and C. J. Weijer. 2005. Paxillin is required for cell-substrate adhesion, cell sorting and slug migration during Dictyostelium development. J. Cell Sci. 118:4295-4310.

9. Chardin, P., S. Paris, B. Antonny, S. Robineau, S. Beraud-Dufour, C. L. Jackson, and M. Chabre. 1996. A human exchange factor for ARF contains Sec7- and pleckstrin-homology domains. Nature 384:481-484.

10. Chen, C. F., and E. R. Katz. 2000. Mediation of cell-substratum adhesion by RasG in Dictyostelium. J Cell Biochem 79:139-149.

11. Chen, L. F., C. Janetopoulos, Y. E. Huang, M. Iijima, J. Borleis, and P. N. Devreotes. 2003. Two phases of actin polymerization display different dependencies on PI(3,4,5)P-3 accumulation and have unique roles during chemotaxis. Mol. Biol. Cell 14:5028-5037.

12. Chen, Y., V. Rodrick, Y. Yan, and D. Brazill. 2005. PldB, a putative phospholipase D homologue in Dictyostelium discoideum mediates quorum sensing during development. Euk. Cell 4:694-702.

13. Cherfils, J., J. Menetrey, M. Mathieu, G. Le Bras, S. Robineau, S. Beraud-Dufour, B. Antonny, and P. Chardin. 1998. Structure of the Sec7 domain of the Arf exchange factor ARNO. Nature 392:101-105.

14. Chernyavsky, A. I., J. Arredondo, L. M. Marubio, and S. A. Grando. 2004. Differential regulation of keratinocyte chemokinesis and chemotaxis through distinct nicotinic receptor subtypes. J Cell Sci 117:5665-5679.

15. Claing, A., W. Chen, W. E. Miller, N. Vitale, J. Moss, R. T. Premont, and R. J. Lefkowitz. 2001. beta-Arrestin-mediated ADP-ribosylation factor 6 activation and beta 2-adrenergic receptor endocytosis. The Journal of biological chemistry 276:42509-42513.

16. Cohen, L. A., A. Honda, P. Varnai, F. D. Brown, T. Balla, and J. G. Donaldson. 2007. Active Arf6 recruits ARNO/cytohesin GEFs to the PM by binding their PH domains. Mol Biol Cell 18:2244-2253.

17. Deakin, N. O., and C. E. Turner. 2008. Paxillin comes of age. J Cell Sci 121:2435-2444.

18. Dormann, D., F. Siegert, and C. J. Weijer. 1996. Analysis of cell movement during the culmination phase of Dictyostelium development. Development 122:761-769.

19. Dormann, D., B. Vasiev, and C. J. Weijer. 2000. The control of chemotactic cell movement during Dictyostelium morphogenesis. Phil. Trans. R. Soc. Lond. B 355:983-991.

20. Duran, M. B., A. Rahman, M. Colten, and D. Brazill. 2009. Dictyostelium discoideum Paxillin Regulates Actin-Based Processes. Protist 160:221-232.

21. Dynes, J. L., A. M. Clark, G. Shaulsky, A. Kuspa, W. F. Loomis, and R. A. Firtel. 1994. LagC is required for cell-cell interactions that are essential for cell-type differentiation in Dictyostelium. Genes Devel. 8:948-958.

22. Eichinger, L., J. A. Pachebat, G. Glockner, M. A. Rajandream, R. Sucgang, M. Berriman, J. Song, R. Olsen, K. Szafranski, Q. Xu, B. Tunggal, S. Kummerfeld, M. Madera, B. A. Konfortov, F. Rivero, A. T. Bankier, R. Lehmann, N. Hamlin, R. Davies, P. Gaudet, P. Fey, K. Pilcher, G. Chen, D. Saunders, E. Sodergren, P. Davis, A. Kerhornou, X. Nie, N. Hall, C. Anjard, L. Hemphill, N. Bason, P. Farbrother, B. Desany, E. Just, T. Morio, R. Rost, C. Churcher, J. Cooper, S. Haydock, N. vanDriessche, A. Cronin, I. Goodhead, D. Muzny, T. Mourier, A. Pain, M. Lu, D. Harper, R. Lindsay, and e. al. 2005. The genome of the social amoeba Dictyostelium discoideum. Nature 435:43-57.

23. Eichinger, L., and F. Rivero. 2006. Methods in Molecular Biology - Dictyostelium discoideum Protocols. Humana Press, Totowa, NJ.

24. Foster, D. A., and L. Xu. 2003. Phospholipase D in cell proliferation and cancer. Mol Cancer Res 1:789-800.

25. Frank, S., S. Upender, S. H. Hansen, and J. E. Casanova. 1998. ARNO is a guanine nucleotide exchange factor for ADP-ribosylation factor 6. The Journal of biological chemistry 273:23-27.

26. Frank, S. R., J. C. Hatfield, and J. E. Casanova. 1998. Remodeling of the actin cytoskeleton is coordinately regulated by protein kinase C and the ADP-ribosylation factor nucleotide exchange factor ARNO. Mol Biol Cell 9:3133-3146.

27. Frohman, M. A., T. C. Sung, and A. J. Morris. 1999. Mammalian phospholipase D structure and regulation. Biochim Biophys Acta 1439:175-186.

28. Haier, J., and G. L. Nicolson. 1999. Role of the cytoskeleton in adhesion stabilization of human colorectal carcinoma cells to extracellular matrix components under dynamic conditions of laminar flow. Clin Exp Metastasis 17:713-721.

29. Hall, A. 1998. Rho GTPases and the actin cytoskeleton. Science 279:509-514.

30. Hernandez-Deviez, D. J., M. G. Roth, J. E. Casanova, and J. M. Wilson. 2004. ARNO and ARF6 regulate axonal elongation and branching through downstream activation of phosphatidylinositol 4-phosphate 5-kinase alpha. Mol Biol Cell 15:111-120.

31. Hoeller, O., and R. R. Kay. 2007. Chemotaxis in the absence of PIP3 gradients. Curr. Biol. 17:813-817.

32. Hofmann, I., A. Thompson, C. M. Sanderson, and S. Munro. 2007. The Arl4 family of small G proteins can recruit the cytohesin Arf6 exchange factors to the plasma membrane. Curr Biol 17:711-716.

33. Huang, C., Z. Rajfur, C. Borchers, M. D. Schaller, and K. Jacobson. 2003. JNK phosphorylates paxillin and regulates cell migration. Nature 424:219-223.

34. Huang, H. J., and C. Pears. 1999. Cell cycle-dependent regulation of early developmental genes. Biochim. Biophys. Acta 1452:296-302.

35. Iyer, S. S., R. S. Agrawal, C. R. Thompson, S. Thompson, J. A. Barton, and D. J. Kusner. 2006. Phospholipase D1 regulates phagocyte adhesion. J Immunol 176:3686-3696.

36. Iyer, S. S., and D. J. Kusner. 1999. Association of phospholipase D activity with the detergent-insoluble cytoskeleton of U937 promonocytic leukocytes. The Journal of biological chemistry 274:2350-2359.

37. Jain, R., I. S. Yuen, C. R. Taphouse, and R. H. Gomer. 1992. A density-sensing factor controls development in Dictyostelium. Genes Devel. 6:390-400.

38. Jermyn, K. A., and J. G. Williams. 1991. An analysis of culmination in Dictyostelium using prestalk and stalk-specific cell autonomous markers. Development 111:779-787.

39. Jiang, Y., H. Levine, and J. Glazier. 1998. Possible cooperation of differential adhesion and chemotaxis in mound formation of Dictyostelium. Biophys. J. 75:2615-2625.

40. Kamboj, R. K., T. Y. Lam, and C. H. Siu. 1990. Regulation of slug size by the cell adhesion molecule gp80 in Dictyostelium discoideum. Cell Regulation 1:715-729.

41. Kessin, R. H. 2001. Dictyostelium - Evolution, cell biology, and the development of multicellularity. Cambridge Univ. Press, Cambridge, UK.

42. Khaire, N., R. Muller, R. Blau-Wasser, L. Eichinger, M. Schleicher, M. Rief, T. A. Holak, and A. A. Noegel. 2007. Filamin-regulated F-actin assembly is essential for morphogenesis and controls phototaxis in Dictyostelium. The Journal of biological chemistry 282:1948-1955.

43. Kimmel, A. R., and R. A. Firtel. 2004. Breaking symmetries: regulation of Dictyostelium development through chemoattractant and morphogen signal-repsonse. Curr. Opin. Genet. Devel. 14:540-549.

44. Kondo, A., S. Hashimoto, H. Yano, K. Nagayama, Y. Mazaki, and H. Sabe. 2000. A new paxillin-binding protein, PAG3/Papalpha/KIAA0400, bearing an ADP-ribosylation factor GTPase-activating protein activity, is involved in paxillin recruitment to focal adhesions and cell migration. Mol Biol Cell 11:1315-1327.

45. Kriebel, P. W., V. A. Barr, and C. A. Parent. 2003. Adenylyl cyclase localization regulates streaming during chemotaxis. Cell 112:549-560.

46. Le Clainche, C., and M. F. Carlier. 2008. Regulation of actin assembly associated with protrusion and adhesion in cell migration. Physiol Rev 88:489-513.

47. Li, C. C., T. C. Chiang, T. S. Wu, G. Pacheco-Rodriguez, J. Moss, and F. J. Lee. 2007. ARL4D recruits cytohesin-2/ARNO to modulate actin remodeling. Mol Biol Cell 18:4420-4437.

48. Li, H. S., K. Shome, R. Rojas, M. A. Rizzo, C. Vasudevan, E. Fluharty, L. C. Santy, J. E. Casanova, and G. Romero. 2003. The guanine nucleotide exchange factor ARNO mediates the activation of ARF and phospholipase D by insulin. BMC Cell Biol 4:13.

49. Lim, C. J., G. B. Spiegelman, and G. Weeks. 2002. Cytoskeletal regulation by Dictyostelium Ras subfamily proteins. J. Muscle Res. Cell Motil. 23:729-736.

50. Liu, C. I., T. L. Cheng, S. Z. Chen, Y. C. Huang, and W. T. Chang. 2005. LrrA, a novel leucine-rich repeat protein involved in cytoskeleton remodeling, is required for multicellular morphogenesis in Dictyostelium discoideum. Dev. Biol. 285:238-251.

51. MacWilliams, H. K., and J. T. Bonner. 1979. The prestalk-prespore pattern in cellular slime molds. Differentiation 14:1-22.

52. Maranda, B., D. Brown, S. Bourgoin, J. E. Casanova, P. Vinay, D. A. Ausiello, and V. Marshansky. 2001. Intra-endosomal pH-sensitive recruitment of the Arf-nucleotide exchange factor ARNO and Arf6 from cytoplasm to proximal tubule endosomes. The Journal of biological chemistry 276:18540-18550.

53. McMains, V. C., X. H. Liao, and A. R. Kimmel. 2008. Oscillatory signaling and network responses during the development of Dictyostelium discoideum. Ageing Res Rev 7:234-248.

54. Mee, J. D., D. M. Tortolo, and M. B. Coukell. 1986. Chemotaxis-associated properties of separated prestalk and prespore cells of Dictyostelium discoideum. Biochem. Cell Biol. 64:722-732.

55. Mondal, S., D. Neelamegan, F. Rivero, and A. A. Noegel. 2007. GxcDD, a putative RacGEF, is involved in Dictyostelium development. BMC Cell Biol. 8:23.

56. Mosavi, L. K., T. J. Cammett, D. C. Desrosiers, and Z. Y. Peng. 2004. The ankyrin repeat as molecular architecture for protein recognition. Protein Sci 13:1435-1448.

57. Myers, S. A., J. W. Han, Y. Lee, R. A. Firtel, and C. Y. Chung. 2005. A Dictyostelium homologue of WASP is required for polarized F-actin assembly during chemotaxis. Mol. Biol. Cell 16:2191-2206.

58. Nagasaki, A., and T. Q. Uyeda. 2007. Screening of genes involved in cell migration in Dictyostelium. Exp. Cell Res.

59. Nanninga, N. 2001. Cytokinesis in prokaryotes and eukaryotes: common principles and different solutions. Microbiol Mol Biol Rev 65:319-333 ; third page, table of contents.

60. Nie, Z., D. S. Hirsch, and P. A. Randazzo. 2003. Arf and its many interactors. Curr Opin Cell Biol 15:396-404.

61. Noegel, A., G. Gerisch, J. Stadler, and M. Westphal. 1986. Complete sequence and transcript regulation of a cell adhesion protein from aggregating Dictyostelium cells. EMBO J. 5:1473-1476.

62. Palsson, E. 2008. A 3-D model used to explore how cell adhesion and stiffness affect cell sorting and movement in multicellular systems. J Theor Biol 254:1-13.

63. Pan, P., E. M. Hall, and J. T. Bonner. 1975. Determination of the active portion of the folic acid molecule in cellular slime mold chemotaxis. J. Bacteriol. 122:185-191.

64. Powner, D. J., M. N. Hodgkin, and M. J. Wakelam. 2002. Antigen-stimulated activation of phospholipase D1b by Rac1, ARF6, and PKCalpha in RBL-2H3 cells. Mol Biol Cell 13:1252-1262.

65. Powner, D. J., T. R. Pettitt, R. Anderson, G. B. Nash, and M. J. Wakelam. 2007. Stable adhesion and migration of human neutrophils requires phospholipase D-mediated activation of the integrin CD11b/CD18. Mol Immunol 44:3211-3221.

66. Prasad, P. D., J. A. Stanton, and S. J. Assinder. 2009. Expression of the actin-associated protein transgelin (SM22) is decreased in prostate cancer. Cell Tissue Res.

67. Rifkin, J. L. 2001. Folate reception by vegetative Dictyostelium discoideum amoebae: Distribution of receptors and trafficking of ligand. Cell Motil. Cytoskel. 48:121-129.

68. Rudge, S. A., and M. J. Wakelam. 2009. Inter-regulatory dynamics of phospholipase D and the actin cytoskeleton. Biochim Biophys Acta 1791:856-861.

69. Sameshima, M., Y. Kishi, M. Osumi, R. Minamikawa-Tachino, D. Mahadeo, and D. A. Cotter. 2001. The formation of actin rods composed of actin tubules in Dictyostelium discoideum spores. J Struct Biol 136:7-19.

70. Santy, L. C., and J. E. Casanova. 2001. Activation of ARF6 by ARNO stimulates epithelial cell migration through downstream activation of both Rac1 and phospholipase D. J Cell Biol 154:599-610.

71. Santy, L. C., S. R. Frank, J. C. Hatfield, and J. E. Casanova. 1999. Regulation of ARNO nucleotide exchange by a PH domain electrostatic switch. Curr Biol 9:1173-1176.

72. Santy, L. C., K. S. Ravichandran, and J. E. Casanova. 2005. The DOCK180/Elmo complex couples ARNO-mediated Arf6 activation to the downstream activation of Rac1. Curr Biol 15:1749-1754.

73. Saran, S., M. E. Meima, E. Alvarez-Curto, K. E. Weening, D. E. Rozen, and P. Schaap. 2002. cAMP signaling in Dictyostelium - Complexity of cAMP synthesis, degradation and detection. J. Muscle Res. Cell Motil. 23:793-802.

74. Savill, N. J., and P. Hogeweg. 1997. Modelling morphogenesis: From single cells to crawling slugs. J. Theor. Biol. 184:229-235.

75. Schaefer, A. W., V. T. Schoonderwoert, L. Ji, N. Mederios, G. Danuser, and P. Forscher. 2008. Coordination of actin filament and microtubule dynamics during neurite outgrowth. Dev Cell 15:146-162.

76. Schafer, D. A. 2002. Coupling actin dynamics and membrane dynamics during endocytosis. Curr Opin Cell Biol 14:76-81.

77. Schaller, M. D. 2001. Paxillin: a focal adhesion-associated adaptor protein. Oncogene 20:6459-6472.

78. Schmidt, A., and M. N. Hall. 1998. Signaling to the actin cytoskeleton. Annu Rev Cell Dev Biol 14:305-338.

79. Secko, D. M., C. H. Siu, G. B. Spiegelman, and G. Weeks. 2006. An activated Ras protein alters cell adhesion by dephosphorylating Dictyostelium DdCAD-1. Microbiology SGM 152:1497-1505.

80. Sesaki, H., and C. H. Siu. 1996. Novel redistribution of the Ca2+-dependent cell adhesion molecule DdCAD-1 during development of Dictyostelium discoideum. Dev. Biol. 177:504-516.

81. Shmuel, M., L. C. Santy, S. Frank, D. Avrahami, J. E. Casanova, and Y. Altschuler. 2006. ARNO through its coiled-coil domain regulates endocytosis at the apical surface of polarized epithelial cells. The Journal of biological chemistry 281:13300-13308.

82. Siu, C.-H., T. Y. Lam, and A. H. C. Choi. 1985. Inhibition of cell-cell binding at the aggregation stage of Dictyostelium discoideum development by monoclonal antibodies directed against an 80,000-Dalton surface glycoprotein. J. Biol. Chem. 260:16030-16036.

83. Siu, C. H., B. Des Roches, and T. Y. Lam. 1983. Involvement of a cell-surface glycoprotein in the cell-sorting process of Dictyostelium discoideum. Proc. Natl. Acad. Sci. USA 80:6596-6600.

84. Siu, C. H., T. J. C. Harris, J. Wang, and E. Wong. 2004. Regulation of cell-cell adhesion during Dictyostelium development. Semin. Cell Dev. Biol. 15:633-641.

85. Sussman, M. 1987. Cultivation and synchronous morphogenesis of Dictyostelium under controlled experimental conditions. Meth. Cell Biol. 28:9-29.

86. Tang, L., R. Ammann, T. Gao, and R. H. Gomer. 2001. A cell number-counting factor regulates group size in Dictyostelium by differentially modulating cAMP-induced cAMP and cGMP pulse sizes. J. Biol. Chem. 276:27663-27669.

87. Tsubouchi, A., J. Sakakura, R. Yagi, Y. Mazaki, E. Schaefer, H. Yano, and H. Sabe. 2002. Localized suppression of RhoA activity by Tyr31/118-phosphorylated paxillin in cell adhesion and migration. J Cell Biol 159:673-683.

88. Turner, C. E., and M. C. Brown. 2001. Cell motility: ARNOand ARF6 at the cutting edge. Curr Biol 11:R875-877.

89. van Haastert, P. J. M., and P. N. Devreotes. 2004. Chemotaxis: signalling the way forward. Nature Rev. Mol. Cell Biol. 5:626-634.

90. Vasiev, B., and C. J. Weijer. 1999. Modeling chemotactic cell sorting during Dictyostelium discoideum mound formation. Biophys. J. 76:595-605.

91. Vitale, N., S. Chasserot-Golaz, and M. F. Bader. 2002. Regulated secretion in chromaffin cells: an essential role for ARF6-regulated phospholipase D in the late stages of exocytosis. Ann N Y Acad Sci 971:193-200.

92. Vitale, N., S. Chasserot-Golaz, Y. Bailly, N. Morinaga, M. A. Frohman, and M. F. Bader. 2002. Calcium-regulated exocytosis of dense-core vesicles requires the activation of ADP-ribosylation factor (ARF)6 by ARF nucleotide binding site opener at the plasma membrane. J Cell Biol 159:79-89.

93. Wang, F. 2009. The signaling mechanisms underlying cell polarity and chemotaxis. Cold Spring Harbor Perspect Biol 1:a002980.

94. Wang, J., L. S. Hou, D. Awrey, W. F. Loomis, R. A. Firtel, and C. H. Siu. 2000. The membrane glycoprotein gp150 is encoded by the lagC gene and mediates cell-cell adhesion by heterophilic binding during Dictyostelium development. Dev. Biol. 227:734-745.

95. Weijer, C. J. 2004. Dictyostellium morphogenesis. Curr. Opin. Genet. Devel. 14:392-398.

96. Wilkins, A., J. Chubb, and R. H. Insall. 2000. A novel Dictyostelium RasGEF is required for normal endocytosis, cell motility and multicellular development. Curr. Biol. 10:1427-1437.

97. Willard, S. S., and P. N. Devreotes. 2006. Signaling pathways mediating chemotaxis in the social amoeba, Dictyostelium discoideum. Eur. J. Cell Biol. 85:897-904.

98. Williams, R. S., K. Boeckeler, R. Graf, A. Muller-Taubenberger, Z. Li, R. R. Isberg, D. Wessels, D. R. Soll, H. Alexander, and S. Alexander. 2006. Towards a molecular understanding of human diseases using Dictyostelium discoideum. Trends Mol. Med. 12:415-424.

99. Wittmann, T., and C. M. Waterman-Storer. 2001. Cell motility: can Rho GTPases and microtubules point the way? J Cell Sci 114:3795-3803.

100. Wong, E., C. Z. Yang, J. Wang, D. Fuller, W. F. Loomis, and C. H. Siu. 2002. Disruption of the gene encoding the cell adhesion molecule DdCAD-1 leads to aberrant cell sorting and cell-type proportioning during Dictyostelium development. Development 129:3839-3850.

101. Woznica, D., and D. A. Knecht. 2006. Under-agarose chemotaxis of Dictyostelium discoideum. Meth. Mol. Biol. 346:311-325.

102. Xu, X. Z., M. V. Garcia, T. Y. Li, L. Y. Khor, R. S. Gajapathy, C. Spittle, S. Weed, S. R. Lessin, and H. Wu. 2009. Cytoskeleton alterations in melanoma: aberrant expression of cortactin, an actin-binding adapter protein, correlates with melanocytic tumor progression. Mod Pathol.

103. Yamauchi, J., Y. Miyamoto, T. Torii, R. Mizutani, K. Nakamura, A. Sanbe, H. Koide, S. Kusakawa, and A. Tanoue. 2009. Valproic acid-inducible Arl4D and cytohesin-2/ARNO, acting through the downstream Arf6, regulate neurite outgrowth in N1E-115 cells. Exp Cell Res.

104. Zouwail, S., T. R. Pettitt, S. Dove, M. Chibalina, D. J. Powner, L. Haynes, M. J. O. Wakelam, and R. H. Insall. 2005. Phospholipase D activity is essential for actin localization and actin-based motility in Dictyostelium. Biochem. J. 389:207-214.